A STUDY ON THE PROCESSING CHARACTERISTICS AND REINFORCING POTENTIAL OF NATURAL FIBER MATS

A Thesis
Submitted to the Graduate Faculty
of the
North Dakota State University
of Agriculture and Applied Science

By

Michael John Ehresmann

In Partial Fulfillment
for the Degree of
MASTER OF SCIENCE

Major Department:
Mechanical Engineering

March 2012

Fargo, North Dakota

North Dakota State University
Graduate School

Title

A Study on the Processing Characteristics and Reinforcing Potential of Natural Fiber Mats

By

Michael Ehresmann

The Supervisory Committee certifies that this ***disquisition*** complies with North Dakota State University's regulations and meets the accepted standards for the degree of

MASTER OF SCIENCE

SUPERVISORY COMMITTEE:

Dr. Chad A. Ulven
Chair

Dr. Alan R. Kallmeyer

Dr. Long Jiang

Dr. Scott W. Pryor

Approved:

4/5/2012
Date

Dr. Alan R. Kallmeyer
Department Chair

ABSTRACT

Limited information exists regarding the processing parameters and extent of reinforcing potential natural fibers have in polymer matrices. The five natural fiber mats studied were low shive flax, mid shive flax, high shive flax, hemp and kenaf. The parameters characterized were fiber size, wax content, surface contact angle, and shive content. The compressive force and unsaturated permeability was measured for each mat, and composites were constructed and tested using selected mats in a soy-based polyurethane (PU) matrix. All mats exhibited a viscoelastic behavior under compression, and an increase in shive content correlated with an increase in relaxation. The presence of shive and larger fiber size increased the permeability. Higher wax content and contact angle lowered the permeability. The mechanical properties for all composites performed better than the neat PU, showing there was matrix to fiber adhesion and load transfer. Hemp outperformed the other fibers studied in all mechanical tests.

TABLE OF CONTENTS

LIST OF TABLES

LIST OF FIGURES

CHAPTER 1. INTRODUCTION

Natural fibers are increasingly being used as a replacement for more conventional fiber reinforcements in polymer matrix composites due to cost savings, reduction in weight, and environmental considerations of using renewable materials. These materials have been found to have acceptable mechanical properties, significant processing advantages, chemical resistance, and a low cost/low density ratio [1]. One study of natural fiber reinforced composites found that natural fiber production results in lower environmental impacts compared to glass fiber production by tabulating the nonrenewable energy requirements for producing a glass fiber mat versus a flax fiber mat. It was found that the glass fiber mat required 54.7 MJ/kg, while the flax fiber mat required only 9.55 MJ/kg. Also, natural fiber reinforced composites have higher fiber content for equivalent performance, which reduces the amount of more polluting matrix polymers, and lower weight of natural fiber reinforced composites improves fuel efficiency in transportation applications [2].

In addition to the advantages posed by natural fibers, it is equally important to study them because of the inherent variation present in natural materials, and in the processing of natural materials. It is then important to understand the effects these variations have on processing parameters and final mechanical properties of their composites [3]. By understanding the causes and effects of the variation, parameters can be optimized to produce improved materials, designed for both processing and performance.

1.1. Natural Fibers

Natural fibers possess several advantages over mineral fibers including low cost, high toughness, low density, good specific strength, low abrasion, reduced skin irritation, reduced tool wear due to non-abrasive qualities, CO_2 neutral when disposed of by burning, biodegradability, as well as good acoustic and thermal insulation performance [1]. Several of these qualities including density, specific strength, and acoustic and thermal insulation properties can be attributed to the structure of natural fibers.

The different types of natural fibers consist of bast, leaf, seed, and fruit. Examples of bast fibers are flax, hemp, kenaf, jute, and ramie. Examples of leaf fibers are pineapple, banana, and sisal. Seed fibers consist of cotton and kapok while an example of a fruit fiber is coir fiber from a coconut. Bast and leaf fibers are most commonly used in composite materials [1]. Table 1 shows the properties of some of the most common natural and manmade fibers.

Table 1: Comparative Properties of Natural and Man-Made Fibers [4] [5].

Fiber	Density (g/cm3)	Tensile Strength (Mpa)	Young's Modulus (Gpa)	Elongation to Break (%)
Cotton	1.5-1.6	287-800	5.5-12.6	7.0-8.0
Jute	1.3-1.45	393-773	12-26.5	1.16-1.5
Flax	1.3-1.5	345-1100	50-70	2.7-3.2
Hemp	1.3-1.5	690	30-60	1.6
Ramie	1.5	400-938	61.4-128	1.2-3.8
Sisal	1.5	468-640	9.4-22.0	3-7
Coir	1.2	131-175	4-6	15-40
E-Glass	2.5	2000-3500	70	2.5
S-Glass	2.5	4570	86	2.8
Aramid	1.4	3000-3150	63-67	3.3-3.7
Carbon	1.7	4000	230-240	1.4-1.8

From Table 1 it can be seen that the bast fibers have the best mechanical properties compared to other natural fibers, and several bast fibers have similar stiffness to E-glass. Other than mechanical properties, another advantage of using a bast fiber such as flax is that it can be grown as a co-product from seed flax. This allows the grower to harvest and sell a by-product of the flax seed growing process, which would otherwise be a waste.

1.1.1. Bast Fibers

Bast fibers are natural fibers which are harvested from a plant stalk. These fibers surround a woody core and are covered by a thin cover called the cuticle or epidermis as seen in Figure 1. These fibers exist in bundles, and must be removed from the other parts of the stalk in order to be used effectively in composite materials. The fibers are located in the sclerenchyma shown in the cross section of the flax stalk in Figure 1 [6].

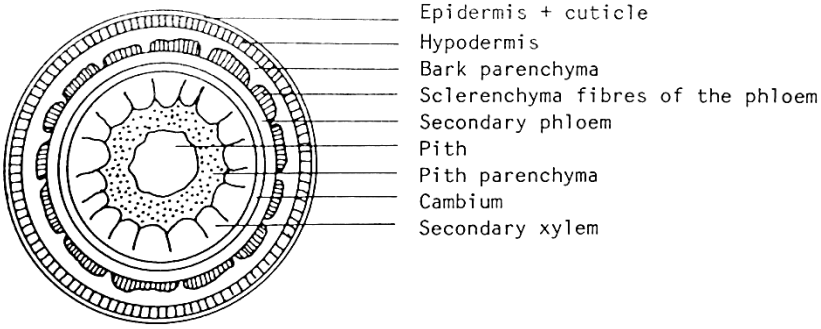

Figure 1: Section of a flax stem [6].

The process of separating the fiber from the woody core and the cuticle is called retting. One such method is known as water retting, which is a process where the flax stalk is fermented and anaerobic bacteria break down the stalk to free the fibers. This process

produces a high quality fiber but the fermentation waste is deemed environmentally unacceptable and so this method is no longer used [7].

Field retting, or dew retting, is considered more environmentally favorable. This process simply leaves the stalk of the plant in the field following harvest, allowing natural moisture and bacteria to break down the stalk. This process does not produce as high of a quality fiber as the fermentation process, but it does not produce the fermentation waste. Field retting can also introduce significant variation into the processing of natural fiber depending on the local climate and weather patterns, and it can tie up production in a field, preventing other crops from being grown. Following retting, the fibers are mechanically separated from the rest of the stalk. Due in part to the non-ideal retting process, it can be more difficult to separate all of the woody material from the fiber, and ultimately some can remain with the fiber [8].

Another retting method currently under development is called enzyme-retting. This process involves the application of water and specific enzymes to break down the cuticle and woody core material, followed by controlled application of temperature and humidity. This method is much more controllable compared to field retting, and it produces less waste than water retting [9].

Bast fibers are the strongest of natural fibers largely due to the high degree of polymerization, high cellulose content and low microfibrillar angle (spiral angle). Table 2 is a list of the composition and spiral angle for the three fibers examined in this study. These properties, however, do not exclusively determine the strength of the fiber. Additional characteristics affecting the properties of natural fibers include source, age, separation or decortication method, moisture content, etc [4]. The acceptable mechanical

properties as well as the large number of potential sources of variation for natural fibers justify further study of these materials.

Table 2: Composition of Bast Fibers [4].

	Cellulose (wt.%)	Hemi-Cellulose (wt.%)	Lignin (wt.%)	Pectin (wt.%)	Wax (wt.%)	Spiral Angle (deg.)	Moisture Content (wt.%)
Flax	71	18.6-20.6	2.2	2.3	1.7	10	10
Hemp	70.2-74.4	17.9-22.4	3.7-5.7	0.9	0.8	6.2	10.8
Kenaf	31-39	21.5	15-19	-	-	-	-

1.1.2. Shive, Hurd, or Trash

During the retting process to extract the fiber from the stems of bast fiber plant, a byproduct is created called shive, hurd, or trash. The name of the byproduct is dependent on the feedstock. Shive is exclusive to flax, while hurd is exclusive to hemp. Trash is a universal term. Trash consists of the woody core material from the stem, shown in Figure 2, which has been separated from the fiber. It is difficult to separate all of the trash from the fiber, and so it is often found mixed with fiber mats in some quantity.

When placed in a polymer matrix composite, the trash has limited load transferring capability. In one study comparing various flax fiber types and varying shive size, it was found that large shive particles had an obvious detrimental role in composite strength. The effect on stiffness was not conclusive, but the results showed that the small and medium shive particles may reduce the elastic modulus [10]. The composition of the flax shive is shown below in Table 3. When comparing the composition to that of flax fiber in Table 2, it is found that the cellulose content reduces from 71 wt.% to 53 wt.% and the lignin content increases from 2.2 wt.% to 24 wt.%. Depending on the matrix material, lignin

greatly reduces the elongation at break due to a cohesion loss [11]. These lignified core tissues also have hollow cells which can act to draw moisture into the composite if they are not fully encapsulated by a polymer matrix. From the perspective of strength, stiffness and moisture absorption then, it is ideal to reduce the trash content in natural fibers as much as possible.

Figure 2: Flax shive.

Table 3: Characterization of Flax Shive [12].

	Cellulose (wt.%)	Hemi-Cellulose (wt.%)	Lignin (wt.%)	Extractives (wt.%)	Ash (wt.%)
Flax Shive	53	13	24	1.5	>2

Figure 3 shows a scanning electron micrograph of a cross section of a flax stem, showing the relative arrangement of the bast fiber bundles (F) with the cuticle covered epidermis (arrows) on the outside of the bundle with the lignified core tissues (C) to the inside. It is the lignified core tissues that make up the shive, but the epidermis/cuticle layer

can also be difficult to separate from the fibers [13]. Also, the hollow cellular structure of the shive is very apparent in the figure.

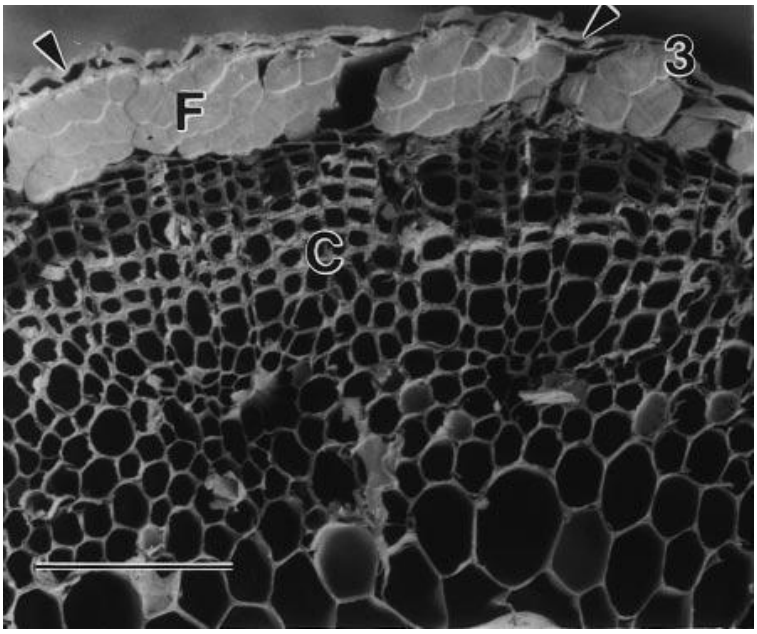

Figure 3: SEM image of cross section of flax stem [13].

1.2. Nonwoven Mats

Nonwoven mats are made from fibers of any type, natural or manmade from fibers of varying length. The fibers in a nonwoven material can be laid out and consolidated in different ways. There are two basic steps to the construction of a nonwoven mat, the first is forming the web, which is basically a loose network of fibers, and the second is bonding of the web [14].

The three basic methods to forming a web are a drylaid system, a wetlaid system, or a polymer based system like a meltblown fabric. All mats in this study were drylaid and so the discussion will focus on this method. For the dry-lay process, bales of fiber are first opened, blended and fed to the web laying machine. There are several different dry-lay processes for producing a web. One process is called carding, where a series of rollers

create a fiber layer from the tangled fiber mass that is fed into the machine. Another process is called the air-lay or aerodynamic web former. This process blows the fibers onto a screen belt in order to form the web [14].

Bonding of the web can be done in several ways, and essentially consolidates the loose collection of fibers in the web into a fabric. This can be done by applying a binder to the web, or by interlocking the fibers mechanically. All of the natural fiber mats examined in this study are interlocked mechanically, and none of them use a binder. Common methods of mechanical interlocking of fibers include needle punching, stitching, and water jet entangling. Needle punching is performed by inserting barbed needles into the web, pulling fibers through the thickness of the web to consolidate it into a mat. A stitch bonding process simply uses threads stitched together to consolidate the web, and the water entanglement works similarly to needle punching, with the difference being high pressure water jets are used to consolidate the web rather than a series of barbed needles [14]. All mats examined in this study were needle punched.

1.3. Permeability

Permeability is the measurement of the ability of a fluid to pass through a porous media. In-plane unsaturated permeability is an essential processing value for modeling the manufacturing of composite materials. It is a value that relates the speed that a fluid front is able to pass through a permeable media to other processing variables [3].

1.3.1. Isotropic Permeability Model

Permeability is a value defined by Darcy's law

$$\mathbf{v}_{\mathrm{D}} = \frac{\mathbf{K}}{\mu}\nabla P \tag{1}$$

where $\mathbf{v}_D$ is the Darcy's velocity vector, P is the pressure, μ is the viscosity, and $\mathbf{K}$ is the permeability tensor. When Darcy's law is combined with the continuity equation

$$\nabla \cdot \mathbf{v}_D = 0 \tag{2}$$

and boundary conditions applied, an equation relating the fluid front to the conditions affecting in-plane radial permeability is found. A graphical representation of important variables for determining this special case for permeability is shown below in Figure 4. The figure shows the inlet gate, which is the location where the test fluid is introduced to the center of the porous media. Also shown is the flow front, where to the inside of this front is the wetted media, and to the outside of this front is the unwetted mat.

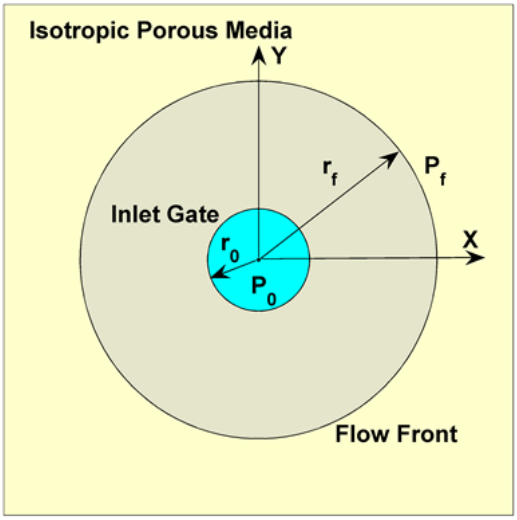

Figure 4: Graphic representation of the isotropic permeability model [15].

This model relates the fluid front position, Φ, to the permeability of the material as well as other test conditions by the equation

$$\Phi(\rho_f) = \tau \tag{3}$$

Where Φ is a function of only the dimensionless fluid front, $\rho_f = r_f/r_o$, where r_f is the fluid front radius and r_o is the inlet gate radius.

Specifically,

$$\Phi(\rho_f) = \frac{1}{4}\left[\rho_f^2\left(2 \cdot \ln\rho_f - 1\right) + 1\right] \tag{4}$$

Permeability and various test conditions are then accounted for by

$$\tau = \frac{k_{xye}\left(P_o - P_f\right)t}{\varepsilon\mu r_0^2} \tag{5}$$

Where k_{xye} is the isotropic in-plane permeability, P_0 is the inlet pressure, P_f is the pressure at the fluid front, t is time, ε is porosity of the mat, and μ is the resin viscosity [15].

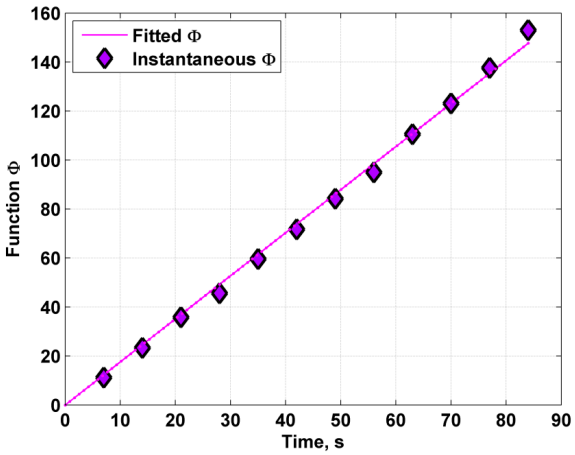

Figure 5: Fitted slope plot.

Additonally, instead of calculating k_{xye} from an instantaneous point during the test, an average value can be used. First, a linear fit can be applied to the Φ vs. t plot to determine the slope m, such that

$$\Phi(\rho_f) = mt \tag{6}$$

and where

$$m = \frac{k_{xye}(P_o - P_f)}{\varepsilon \mu r_0^2} \tag{7}$$

A sample plot demonstrating a linear fit of the data is shown in Figure 5 [15].

1.3.2. Justification for the use of the Isotropic Model

This model was chosen to evaluate the in-plane permeability of the nonwoven mats because there is no preferred direction for the fluid flow, and so the mats are considered to be quasi-isotropic in the in-plane direction. Unidirectional or woven mats exhibit anisotropic permeability behavior and require a more complex model to determine permeability. Figure 6 shows the advancement of the fluid front over a 45 second period. The test shown is representative of all of the tests conducted and for all materials. The fluid front profile maintains a round shape throughout the test, thus indicating no preferred direction and justifying the isotropic model.

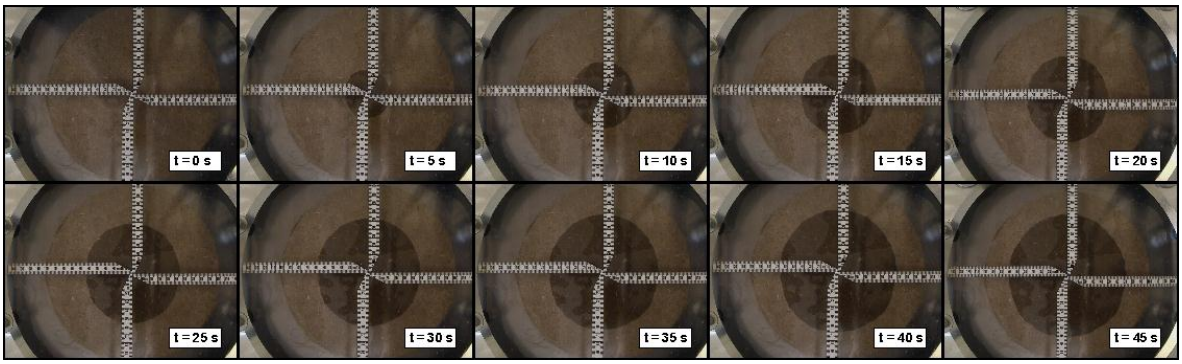

Figure 6: Series of pictures for the test of the hemp mat with 250 cP oil and Vf = 0.30.

1.4. Wettability

Wettability is a measurement of the interaction between a liquid and a solid, and for the purpose of this study was used to measure the interaction between the natural fibers and the simulated resins. Wettability measurements between a fiber and a matrix are often used for composite materials to examine the interfacial adhesion, particularly for the use of fiber surface modification studies [16] [17]. Wettability is also important for composite manufacturing since resin – fiber combinations with poor wettability can lead to void formation during impregnation [18]. Voids in the matrix can result in a loss of mechanical properties, which also stresses the importance of an understanding of the fluid – fiber interaction. The interest in wettability for this study, however, is to compare the influence of the fluid – fiber interaction on permeability.

Contact angle can be used to calculate a value for surface energy for a solid by the Young-Dupres equation where the solid surface energy (γ_s) can be found by:

$$\gamma_S = \gamma_{SL} + \gamma_L cos\ \theta \tag{8}$$

where γ_{SL} and γ_L are the energies for the solid liquid interface and the liquid surface, respectively. θ denotes the contact angle of the liquid on the solid. This equation applies to perfectly smooth, chemically homogeneous surfaces, which clearly cannot be applied to natural fibers [19]. This equation is mentioned to illustrate that a smaller contact angle will mean a larger solid surface energy. A large free surface energy will increase the adhesion properties of the solid and increase the wettability [20]. Conversely, a large contact angle will lead to a low surface energy, and is associated with poor wettability.

There are several well established methods for examining the interaction of a solid and a fluid. These include the contact angle goniometry, capillary rise method, the Wilhelmy method, and atomic force microscopy. Contact angle goniometry is the measurement of contact angle of a droplet on a fiber or other solid material. The droplet is backlit and an image is then captured. From the image, contact angle is measured either manually with an optical goniometer or automatically with image analysis software [21]. The image of a backlit epoxy resin droplet on a sisal fiber is shown in Figure 7.

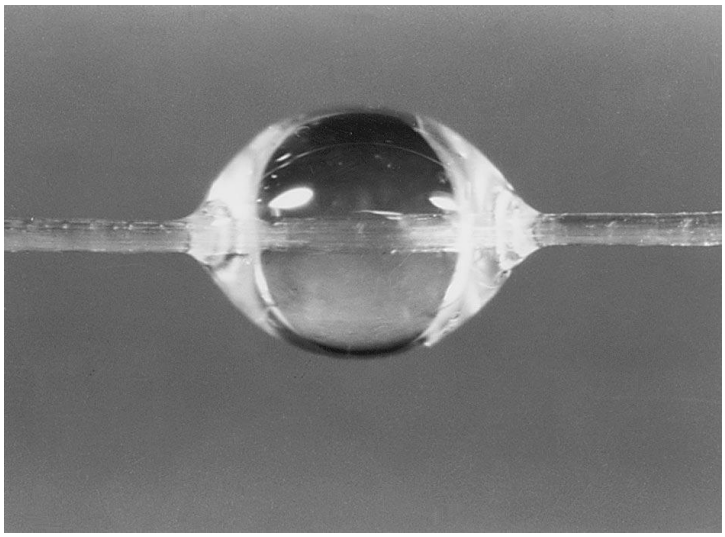

Figure 7: An epoxy drop attached to a monofilament sisal fiber [20].

Another consideration for wettability and resin impregnation is capillary pressure, which is a driving force for liquids passing through a dry medium. Capillary pressure is also commonly known as wicking, and can aid the impregnation and processability of the composite. It is particularly important where low pressures are used to force the resin through an unwetted fiber preform, which causes capillary pressure to become a more dominant flow driver [22]. Capillary pressure was not measured in this study and all

permeability experiments were conducted using 101 kPa ΔP, but it is an important consideration that will be discussed later.

1.5. Compression of Nonwoven Fibers

Fiber networks are almost always compressed to some degree during the fabrication of composite materials to achieve a desired fiber volume fraction. The compression of fiber networks require an applied pressure, which increases with an increase in fiber volume fraction, and with some fibers this compressive force can relax over time. It is important then to understand the effects of compression for the consideration of both applied pressure for mold design, as well as relaxation time required prior to resin infusion.

Typically, compressive pressure is plotted versus fiber volume fraction, as shown in Figure 8. This figure shows the compressive pressure (stress) compared to the fiber volume fraction for several different fiber types and orientations. Note that the random mat requires a much higher compressive force than unidirectional or woven rovings to achieve the same fiber volume fraction. The random mat tested in this particular study was a fiberglass random mat manufactured by Bean Glass Fiber, Inc. It was the conclusion of this study that force versus fiber volume fraction was dependent on both the fiber orientation and the stacking method [23]. Fiber volume fraction is the ratio of volume of fiber divided by the total volume of the composite, resulting in a fraction. All fiber volume fractions in this study are reported as a percentage, which is found by multiplying the fraction by 100 %.

Relaxation of a fiber network is observed by compressing the fibers to the desired fiber volume fraction, and then observing the decrease in compressive force over time. In the same study Figure 9, shows a reduction of the stress/initial stress equal to 0.75 over a period of 300 seconds for the same fiberglass random mat. Relaxation was dependent on

fiber orientation, span length and fiber breakage during compression. Random mats exhibited the greatest relaxation, and relaxation decreased with fiber orientation. The data for stress relaxation correlated well with a Maxwell-Weichert viscoelastic model [23].

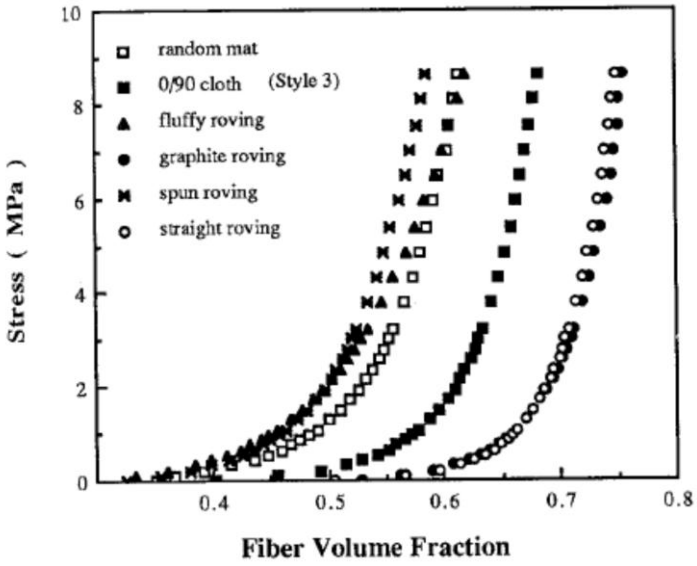

Figure 8: Effect of fiber orientation on compressibility [23].

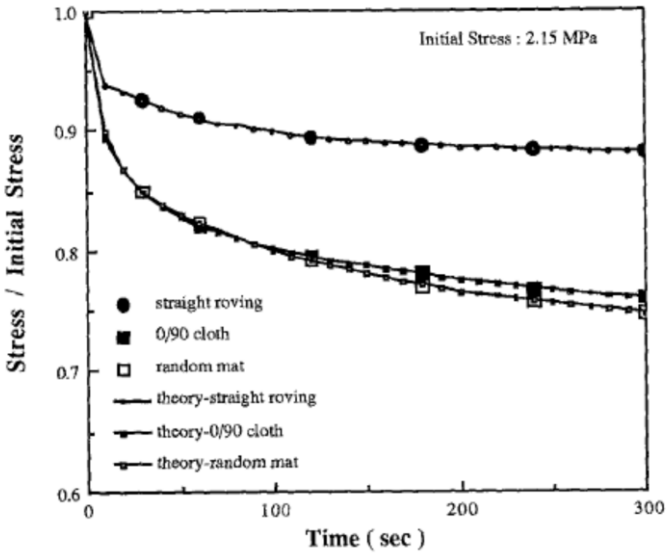

Figure 9: Effect of fiber orientation on stress relaxation [23].

CHAPTER 2. OBJECTIVE

Natural fibers are increasingly used in fiber reinforced composite materials to replace fiberglass due to cost savings, weight reduction, and utilizing renewable materials. The purpose of this study was to evaluate the processing behavior and reinforcing potential of various natural fiber mats. There were two objectives of this research, the first was to characterize mat processing qualities such as relaxation under compression and permeability, and correlate these properties to fiber specific properties. The second objective of this research was to characterize natural fiber reinforced soy-based polymer composites using several different fibers to prove the load transfer capability of different natural fibers.

The reason for relating processing variables to fiber properties is due to the large number of variables associated with the production of natural fibers. For example, some of the variables that could affect the fibers are the growing conditions, retting method, decortication method, source of the fiber, etc. By focusing on properties such as fiber size, wax content, wettability, and shive content, the processor can test the material and know what to expect regarding processing, rather than attempt to control all steps of the fiber production process. Also, by understanding the effect of measurable fiber properties, it allows the grower and fiber processor to adjust their procedures to produce a particular quality of fiber.

2.1. Experimental Goals

- Determine the fiber characteristics including fiber size, wax content, fiber density and wettability.

- Determine the mat properties including shive content, relaxation under compression, areal density, and permeability.
- Measure the mechanical properties of natural fiber reinforced soy-based polyurethane composites.

2.2. Analytical Goals

- Compare permeability data to determine effect of wettability, shive content, fiber size, wax content, and resin viscosity.
- Compare permeability data to determine the effect of fiber volume fraction.

2.3. Intended Outcome

The purpose of this study was to better understand the processing characteristics of natural fiber mats for use in fiber reinforced composite materials and make recommendations to natural fiber mat processors and natural fiber reinforced composite manufacturers on how to optimize for best performance.

CHAPTER 3. MATERIALS

The materials examined in this study include five different nonwoven mats made from flax, hemp and kenaf fibers. All of the fiber types examined in this study are bast type fibers extracted from plants. None of the fibers from this study underwent surface treatments to improve interfacial bonding properties. Three different flax mats are examined; a low shive content mat, a mid shive content mat, and a high shive content mat. The hemp and kenaf mats are both considered to have low woody core content.

3.1 Low Shive Flax Mat

The low shive flax mat used for this study was provided by the Composites Innovation Centre. It is a nonwoven, needle punched mat that contains some shive. Figure 10 shows a backlit sample of the mat. The light areas show localized areas of reduced areal density. The specification for the average areal density of the mat is 500 gsm and an average thickness of 6.50 mm.

Figure 10: Backlit low shive flax mat.

The fiber used for the mat was Manitoba grown oil seed flax and it was winter retted. The nonwoven mat was manufactured by Federal-Mogul Systems Protection of Exton, PA. The bales were processed through a picker to mix the fibers and reduce the variation in the fibers from bale to bale. The web was formed using a Rando Air Laid Machine with a dust collection system. The mat was needle punched using a Fefrer down-stroke needle punch machine.

3.2 Mid Shive Flax Mat

The mid shive flax mat is a cross laid needle punched nonwoven flax fiber mat containing some shive. It was provided by the Composites Innovation Centre. A backlit sample of the mat is shown in Figure 11. The light areas show localized areas with a reduced areal density. This mat appears to be much more consistent than the low shive flax mat, but some of this is likely due to the higher areal density (there was no areal density specification for this mat) of the mid shive flax mat.

Figure 11: Backlit mid shive flax mat.

3.3 High Shive Flax Mat

The high shive flax mat utilized for this study is not designed for the purpose of use in composite materials, but is rather produced for use as ground erosion prevention. It is however a nonwoven flax fiber mat with a high shive content, and ideal for use in this study to determine the effect of shive.

A backlit sample of the high shive flax mat is shown below in Figure 12. Note the variation in areal density as seen by light penetrating the mat. Less light penetrates the high shive flax mat than the low shive flax mat due to the higher areal density (there was no areal density specification for this mat) of the high shive flax mat.

Figure 12: Backlit high shive flax mat.

3.4 Hemp Mat

The production of the hemp mat used in this study was coordinated by the Composites Innovation Centre of Winnipeg, Manitoba. The hemp fiber was sourced from Stemergy Renewable Fibre Technologies of Delaware, Ontario. The mat manufacturing trial was performed by Federal-Mogul. The result was a 100% hemp fiber non-woven mat with an

average areal density of approximately 500 gsm. A picture of the final roll is shown below in Figure 13.

Figure 13: Hemp mat roll.

The hemp fibers were collected from straw with a fiber variety of Uniko – B. The fibers were grown Southwest of London, Ontario in the year 2000. The straw was cut in the month of August and was field retted for one month prior to being baled.

The mat was manufactured using the Federal-Mogul R & D nonwoven production line. The equipment in the line includes an opening to feed fibers which is capable of blending up to five different fiber types, an airlay webber, a needle punch, a thermobonding unit, a unit for applying mat treatments or coatings, a mat trimmer, slitter, and roller. The line can produce up to an 200 cm wide mat, but the hemp mat was made 127 cm wide.

The bales were processed through a picker to mix the fibers and reduce the variation in the fibers from bale to bale. The web was formed using a Rando Air Laid Machine with a dust collection system using a run speed of 4 meters per minute. The mat was needle punched using a Fefrer down-stroke needle punch machine with a needle punch density of 15.5 per square cm.

It was determined during mat production that due to the low moisture content of the fiber and the relatively large fiber size of the hemp fibers created difficulties in feeding of the fibers and the creation of the initial web. The use of a water mist reduced the feeding issues, but there were still some issues which led to variations in the areal density, including thin spots. It was stated that the feeding issues could be addressed by setting up the line to specifically process bast fibers, but could not be done for the test run. Some of these thin spots are clearly visible in Figure 14.

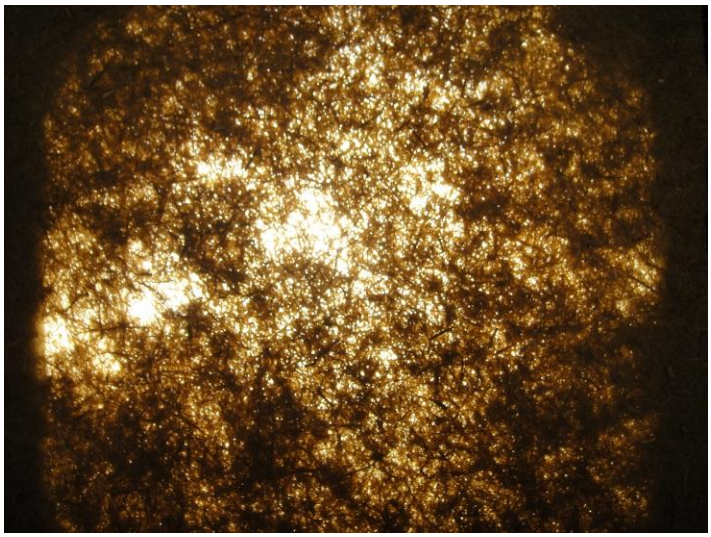

Figure 14: Backlit hemp mat.

3.5 Kenaf Mat

The Kenaf mat used in this study was provided by the Composites Innovation Centre. The mat is a cross laid, needle punched nonwoven mat with a specified average areal density of 500 gsm. Figure 15 shows a backlit sample of the kenaf mat. The figure clearly shows some variation in the areal density present in the mat, as well as some small holes present in the transverse direction due to needle punching of the mat.

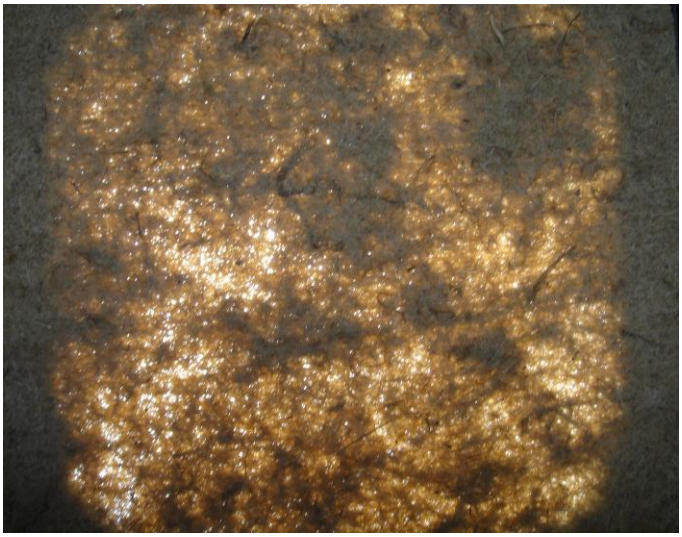

Figure 15: Backlit kenaf mat.

The kenaf fiber was sourced from Bangladesh via Bast Fibers LLC of Creskill, NJ. The nonwoven mat was manufactured by Federal-Mogul on their R & D nonwoven production line. The bales were processed through a picker to mix the fibers and reduce the variation in the fibers from bale to bale. The web was formed using a Rando Air Laid Machine with a dust collection system, and the mat was needle punched using a Fefrer down-stroke needle punch machine.

3.6 Simulated Resins

SAE 40W and SAE 10W-40 were used in lieu of resin systems for the permeability testing. These simulated resins were used due to the cost of resin systems, the need to mix the resins, and the cleanup which would be required to prevent the resin from curing within the permeability apparatus. So the use of these oils provides a low cost fluid that requires no mixing, and the system needs to be cleaned out only when switching from one type of oil to another.

The SAE 40W oil was found to have a viscosity of approximately 400 cP at 20°C, while the SAE 10W-40 was approximately 250 cP at 20°C. Plots of the viscosity versus temperature are shown below in Figure 16 and Figure 17.

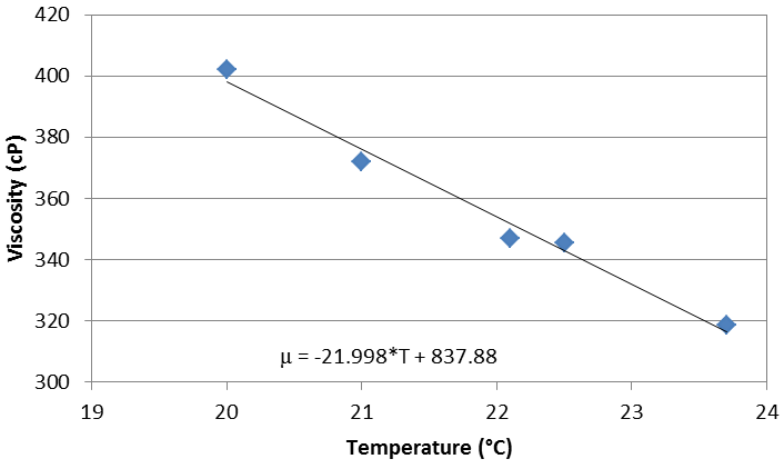

Figure 16: Plot of viscosity versus temperature for SAE 40W.

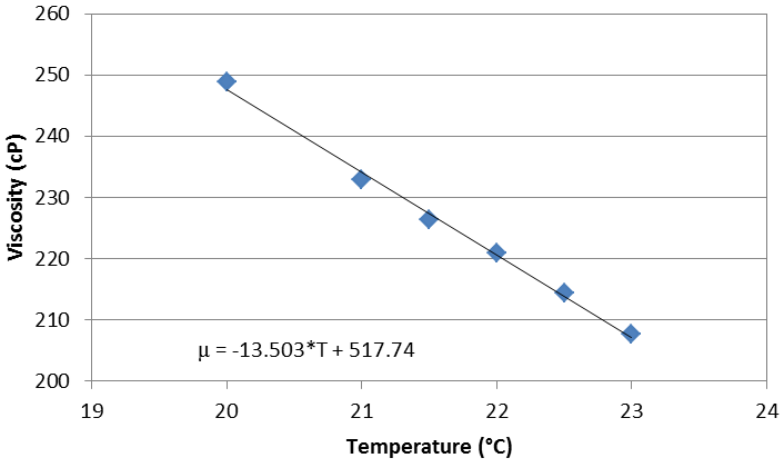

Figure 17: Plot of viscostiy versus temperature for SAE 10W-40.

These two oils were selected to be used as simulated resins due to the similarity of their viscosity to the viscosity of several resins likely to be used with natural fibers. Table 4

below shows a list of these different resins and their mixed viscosities. The epoxy, vinyl ester and polyester are all very similar to the simulated resin viscosities. The soy based polyurethane, however, has a much higher viscosity than either of the simulated resins used in this study.

Table 4: List of Resins and Mixed Viscosities.

Resin	Mixed Viscosity
Epoxy - Huntsman 8601/8602	175 cP
Vinyl Ester - Fiber Glast #1110	275 cP
Polyester - Fiber Glast #77	475 cP
Soy-Based Polyurethane - USS SoyMatrix™	1210 cP

3.7 Soy-Based Polyurethane

For the mechanical testing portion of this investigation, a soy-based polyurethane was reinforced with several of the natural fiber mats. The soy-based polyurethane used is a product called SoyMatrix™ produced by Urethane Soy Systems Company of Volga, SD. SoyMatrix™ is a non-foam, rigid polyurethane, mixed from a two component system. The A-side is a soy-based polyol and the B-side is isocyanate mixed in the ratio of (100:73.4). Since the polyol is soy-based, the final rigid polyurethane consists of approximately 30% renewable feedstock.

CHAPTER 4. EXPERIMENTAL SETUP

In order to understand some of the fiber and mat properties which may influence permeability, a series of tests were performed to characterize the mats and fibers in addition to the permeability and mechanical testing. It is important to characterize the fibers and mats due to the variations in fiber type, processing, and mat construction. The purpose is to characterize variables for natural fibers, and determine what effect, if any, that they have on the permeability and mechanical properties.

The mechanical testing of natural fiber reinforced composites was performed by introducing a soy-based polyurethane matrix. The plaques were formed by compression molding. These plaques were then tested to establish some baseline mechanical properties that could be expected from these materials.

4.1 Density Testing

Density testing of the mats was required to determine the required thickness for a given mat to achieve a desired fiber volume fraction. To determine this required thickness, both the fiber density and the areal density must be known. The thickness is calculated by

$$\delta = \frac{m}{\varepsilon A \rho} \tag{9}$$

Where δ is the thickness, m is the mass of the sample, ε is the desired porosity, A is the area of the sample, and ρ is the fiber density.

4.1.1. Fiber Density

Fiber density was determined for this testing using the Archimedes method. This testing was completed using a Mettler Toledo 33360 Density Determination Kit and

balance. This method is used since the samples can be tested for mass, but the volume of the fiber is unknown. The Archimedes method uses buoyancy to determine the mass of the fiber, and so it is not necessary to know the volume.

The density of the fiber, ρ, is determined by

$$\rho = \frac{m_{dry}}{m_{dry} - m_{wet}} \rho_{fluid} \tag{10}$$

Where m_{dry} is the dry mass of the mat sample, m_{wet} is the mass of the submerged mat sample, and ρ_{fluid} is the density of the immersion fluid. For all mats the immersion fluid used was canola oil.

The sample for each test was a section of each respective mat approximately 1 cm square. Since the sample is taken from the entire mat, the test will measure the density of both the fiber and any shive or trash present in the mat. The result of this is an effective density, which will be used to calculate an effective fiber volume fraction using equation (9).

4.1.2. Areal Density

Areal density is simply a calculation of mass divided by the area. This was done by taking twenty 125 mm x 125 mm samples of each mat, drying them at 80°C for 24 hours, and recording the mass of each mat. The mass for each sample was then recorded at room temperature. The units used for this determination is grams per square meter (gsm), which is a measurement of mass per unit area and a common property referenced for textiles.

4.2 Fiber Property Testing

4.2.1. Wax Content

The wax content of the fibers was determined by the USDA Agricultural Research Station, Cotton Quality Research Station (ARS CQRS) in Clemson, SC using a solvent extraction technique. The sample taken from the mat was fiber only, and did not include any shive or trash present in the mats. Following the solvent extraction the wax content was determined as percentage of the weight.

4.2.2. Fiber Thickness

This testing was performed by the USDA Agricultural Research Station, Cotton Quality Research Station (ARS CQRS) in Clemson, SC. The method used image analysis software called Fibreshape to measure the thickness of the fibers. Fibreshape is used by the USDA ARS CQRS to also measure fiber length, transparency, brightness, and shape factor.

The procedure for measuring first involves placing the fibers between two glass slides, and then a Nikon Super Coolscan 5000 ED 4200 resolution slide scanner captures an image of the fibers between the slides. The image is read from the slide scanner using Silverfast® Ai Studio Version 6.5 Professional Scanner Software and then imports the image into Adobe® Photoshop®. The image is then imported into Fibreshape for analysis.

4.3. Shive Content Testing

Shive content of the flax mats was determined by the Composites Innovation Centre, Inc. using a near infrared (NIR) spectroscopy method. The equipment used is a Polychromix Phazir, which is a portable NIR device calibrated with a partial least squares method (PLS) prediction model that correlates the weight fraction of shive in decorticated

flax fiber to its near infrared spectrum. The sample is prepared for this method by grinding a sample of the whole mat, and the ground material is then analyzed using the Polychromix Phazir.

4.4. Compression Testing

Compression testing was completed using an Instron Model 5567 load frame with a 30 kN load cell. The samples were first dried at 80°C for 24 hours, and the testing was performed in a lab at room temperature. The samples were compressed between two aluminum plates, as show below in Figure 18. The test was completed by first bringing the two aluminum plates together and zeroing the gage length. The crosshead was then raised and the load was zeroed. A test sample was then inserted between the two flat plates, and a preload of 10 N was placed on the sample.

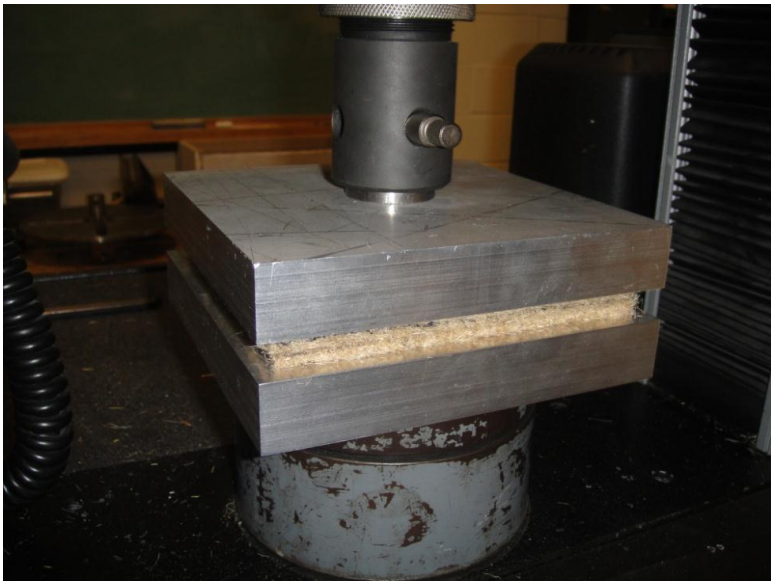

Figure 18: Compression test setup.

The sample area for each test was 125 mm x 125 mm. The test was then initiated with a constant crosshead rate of 3 mm/min, until the sample was compressed to the desired

thickness. The thickness was determined by calculating the required thickness to achieve the desired fiber volume fraction. Tests were conducted for both a 50% and 20% fiber volume fraction, with three replicates for each test. All five natural fiber mats were tested, as well as a fiberglass continuous fiber mat, in order to compare the results of the natural fiber mats to a mineral fiber mat.

4.5. Permeability Testing

The permeability testing was performed on a custom apparatus designed and built at North Dakota State University for testing the in-plane radial permeability of porous media. The in-plane radial permeability testing is done by introducing the simulated resin at the center of the permeable media and the fluid flow is observed in the in-plane direction. It is assumed with this test setup that the transverse permeability can be ignored.

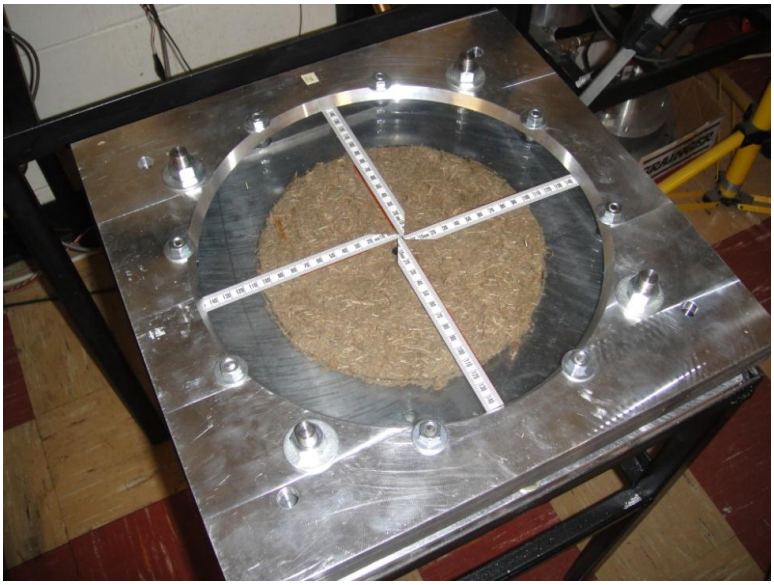

Figure 19: Permeability apparatus.

The basis for the design is such that the permeable media, fiber volume fraction, simulated resin (i.e. simulated resin viscosity), and resin pressure can be varied. The

outputs for the permeability apparatus are simulated resin viscosity and a video of the fluid flow front passing through the permeable media. The video is recorded with the camera viewing the sample through a viewing window with four scales for taking measurements, as shown in Figure 19.

The piping and instrumentation for the permeability apparatus is shown in Figure 20. Starting at the air supply, pressurized air is introduced into the system through the pressure regulator. It is here that the fluid pressure is controlled. All tests for this study were conducted using a pressure setting of 101 kPa to simulate a VARTM manufacturing process. The air tank downstream of the pressure regulator is used as a reservoir to maintain a near constant pressure in the system as the simulated resin volume decreases during each test. The resin tank is simply a tank containing the pressurized simulated resin to be used for the testing. The video camera is setup in order to capture a video testing chamber throughout the test to view the fluid flow front as it passes through the sample. The video is then analyzed offline to record the fluid flow front position. Dual pressure transducers are connected to a data acquisition system to record the simulated resin pressure throughout the duration of the test. The purpose of this is to confirm the fluid pressure, as well as confirm the fluid pressure remained constant throughout the test. The test is initiated by opening the valve between the resin tank and the testing chamber. Once the sample is fully wetted, the valve is closed and the test is ended.

A cross-section view of the testing chamber is shown in

Figure 21. The testing chamber serves several purposes including compressing the sample, aligning the fluid inlet with the center hole of the test sample, maintaining the desired fiber volume fraction, and providing a transparent view window as a means to observe the fluid

flow front. The spacers are used to maintain a desired thickness between the transparent view window and the base plate. The importance of this thickness was discussed in section 4.1 where the thickness of the mat can be calculated to obtain a desired fiber volume fraction. A nut on each of the threaded bolts are then tightened to compress the sample, until the transparent view window and the base plate are both in contact with the spacer and the sample is at the desired thickness.

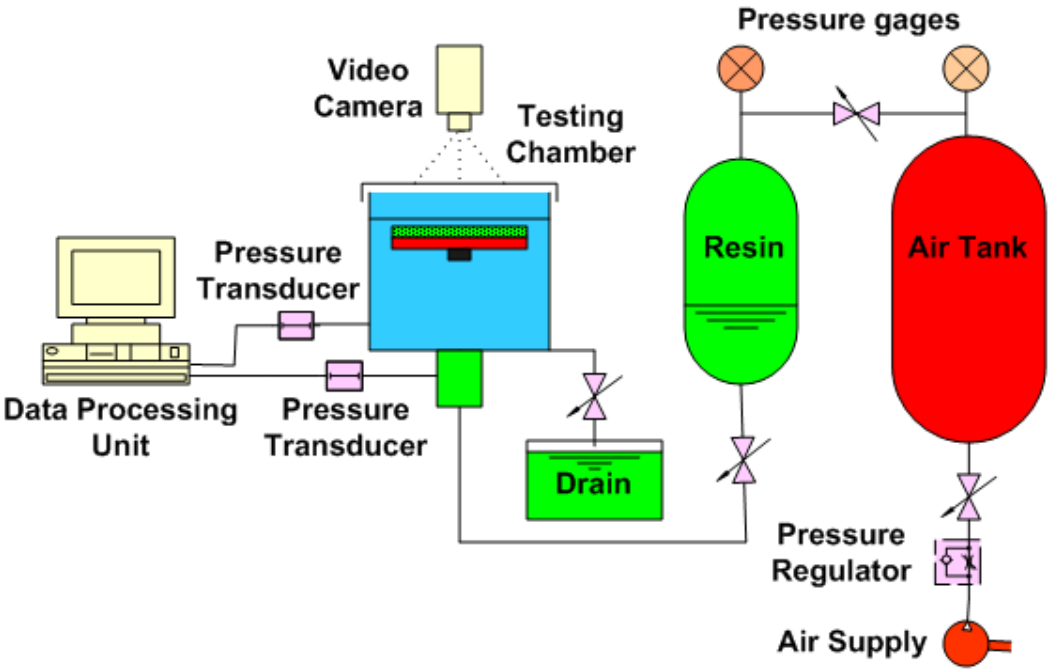

Figure 20: Permeability apparatus piping and instrumentation [3].

All mat samples used for permeability testing were round, and were 150 mm to 300 mm in diameter. The samples were then dried at 80°C for 24 hours prior to testing, they were then allowed to cool to room temperature under lab conditions prior to being installed in the apparatus. The mats were then compressed in the apparatus and allowed to relax prior to infusion.

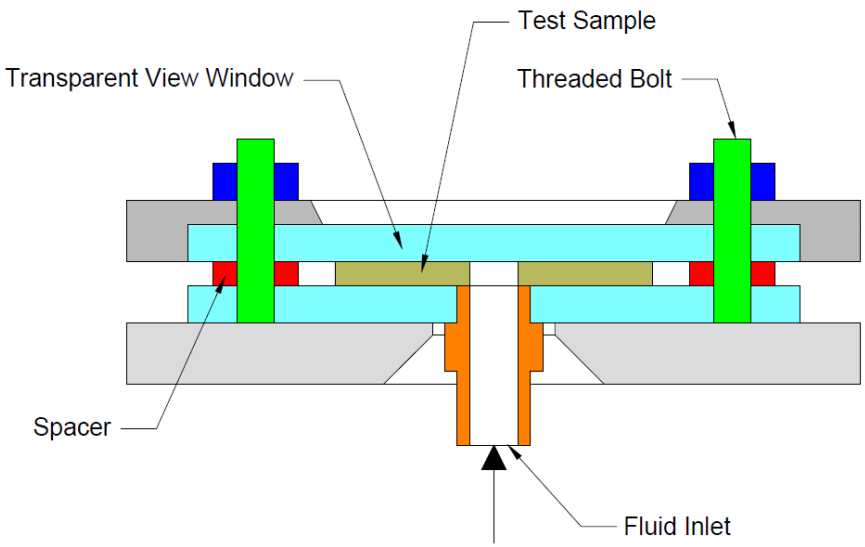

Figure 21: Cross-section of testing chamber.

A frame of the video captured during a test is shown below in Figure 22. Here the sample can be clearly seen through the transparent viewing window, along with the fluid flow front being distinctly visible. Note the four scales located on the transparent viewing window for use in recording the fluid flow front position. In this way the fluid front position is recorded at four different points for each time step. The four measurements were then averaged, resulting in a mean fluid front position used to determine permeability.

The video captured during the testing is then analyzed using Sony Vegas Movie Studio HD Platinum (version 10.0). This software is typically used for editing video, but in this case it is used for its capability to view each individual frame to record the fluid flow front position accurately at a given point in time. The fluid flow front can clearly be seen in the mat shown in Figure 23. For each test, a minimum of eight and a maximum of twelve time steps were used to record the position of the fluid flow front an insure a good fit for the fitted Φ function as shown in Figure 5.

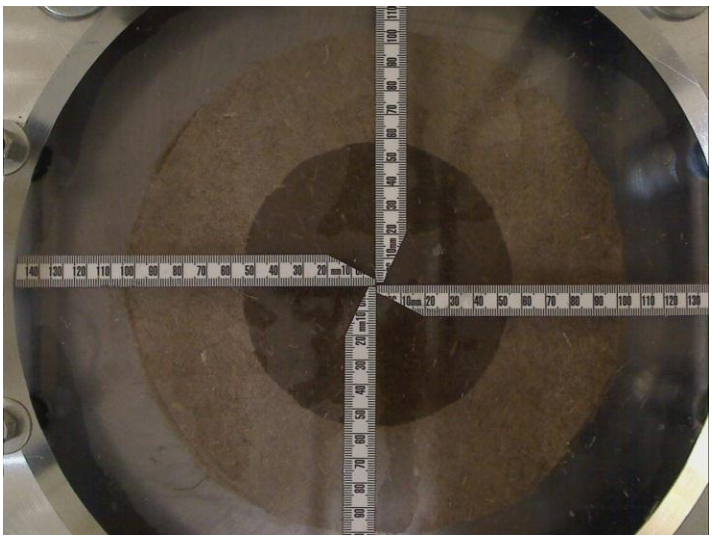

Figure 22: Screenshot of permeability test.

Figure 23: Measurement from video analysis.

4.6. Wettability Testing

Wettability of the natural fiber mats was tested by measuring the contact angle between both simulated resins and the fiber from each mat. This contact angle was measured using a First Ten Angstoms FTA125. To perform the test, a sample of the mat

being tested was first dried at 80°C for 24 hours, and the contact angle testing was performed at room temperature under laboratory conditions. Individual fibers were extracted from the respective mat, and were then mounted so the droplet could be suspended on the fiber, as seen in Figure 7. Multiple oil droplets were then placed on the fiber, and the contact angle was measured for each. This was repeated for several fibers from each mat. Figure 24 shows a typical contact angle measurement as measured by the FTA 125. This procedure was replicated for all five mats, with both simulated resins. This test then is a characterization of the hydrophilic fiber and the hydrophobic resin (or oil), and it is specific to that particular fluid/fiber interaction.

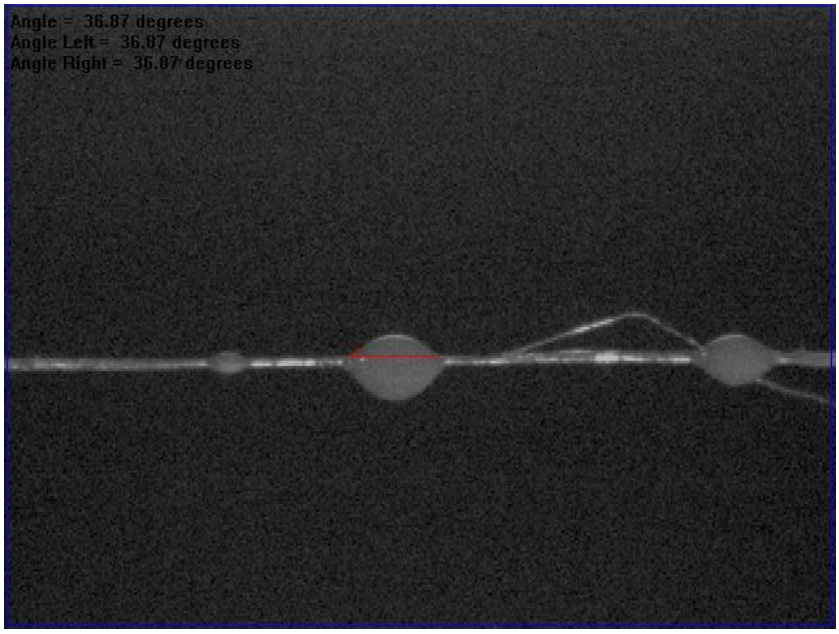

Figure 24: Image captured from contact angle testing.

It should be mentioned that this test method does not account for the wettability of the shive present in the mats. To perform a wettability test which would account for shive in the mat, the mat and the shive would need to be tested as one. Attempts were made to

measure the contact angle between the simulated resin and a sample of the mat, but the applied droplet would wick into the mat, making a contact angle measurement impossible.

Shive wettability was tested separately in a similar manner as the fibers, where an oil droplet was placed on the shive sample taken from each of the three flax mats. Due to the short length of most of the shive, it was place on a flat surface for testing, rather than suspending the sample. An oil droplet was then placed on top of the shive, and the contact angle was recorded.

Contact angle testing was also performed on only the low shive flax fiber with several commercial resin systems. The purpose of this testing was to compare the contact angle of the simulated resins with the commercial resins. The resin systems tested were Huntsman 8601/8602 Epoxy, Soy Matrix^{TM} polyurethane, and AOC Resins Hydropel® R037-YDF-40 vinyl ester.

4.7. Mechanical Property Testing

The mechanical properties of compression molded natural fiber reinforced soy-based polyurethane were evaluated to establish baseline performance. Due to limited quantities of some of the mats, this portion of the testing could not be performed on all five mats. The three natural fiber mats tested for their mechanical properties were the low shive flax, kenaf, and hemp mats. The results of the natural fiber reinforced polyurethane were also compared with neat polyurethane. The mechanical tests performed on the samples include tensile, flexural, and izod impact.

4.7.1. Compression Molding

The samples were molded by first cutting and drying multiple layers of each respective mat, and drying the mats at 80°C for at least 24 hours to remove any moisture which would

react with the polyurethane system. To remove moisture from the polyurethane system, the polyol was dried in a vacuum oven at 80 °C and -20 inHg for 24 hours. The processing of the panels was then done at room temperature in laboratory conditions. The SoyMatrix^{TM} system was mixed and poured into the base of the mold, and the dried mats were then placed on top of the polyurethane mix. The mold plug was then placed on top of the mats, and the mold was placed into the press. The pressure applied to the plug forced the mixed resin through the mats, and any excess resin would exit the mold as flash.

Figure 25: Compression mold placed in press.

The press used was a Carver Hydraulic Unit Model 3912. The mold size is 102 mm x 203 mm. A force of approximately 50 kN was applied to the mold area, resulting in a compressive pressure of 2400 kPa. The mold was then held under compression for a minimum of 24 hours to allow the polyurethane to cure.

4.7.2. Tensile Testing

Tensile testing completed in according to ASTM D3039-00. This is the standard test method for tensile properties of polymer matrix composite materials [24]. The tensile tests

were performed in an Instron Model 5567 load frame using a 30 kN load cell at room temperature under laboratory conditions. With an extensometer installed, the sample is placed under 20 MPa of tension, the test is then paused to remove the extensometer, and the sample is tested to failure. The strain information from the extensometer was used to calculate the elastic modulus, and the maximum load achieved was used to determine the ultimate strength.

4.7.3. Flexural Testing

Flexural testing was completed according to ASTM D790. This is the standard test method for flexural properties of unreinforced and reinforced plastics [25]. The test is a three point bend test, and it was performed in an Instron Model 5567 load frame using a 2 kN load cell. The test was performed at room temperature under laboratory conditions. The flexure load and the flexure extension were then used to determine the flexure stress and the flexure strain.

4.7.4. Impact Testing

Impact testing was completed according to ASTM D256. This test method is used to determine the Izod pendulum impact resistance of plastics. The test method used was Test Method A, where the specimen is held vertical and is broken using the single swing of a pendulum, with the pendulum striking the face of the specimen with the notch. The energy in the tossed portion (the part of the sample which is fractured from clamped portion) of the specimen is not taken into account [26].

All specimens were compression molded to a thickness of approximately 5 mm, well within the 3.0 mm to 12.7 mm specification in the standard [26]. The individual specimens were then cut from each plaque and notched. The specimens were then dried and tested

using a Tinius Olson Izod Impact test machine, shown in Figure 26. The test was performed at room temperature under laboratory conditions.

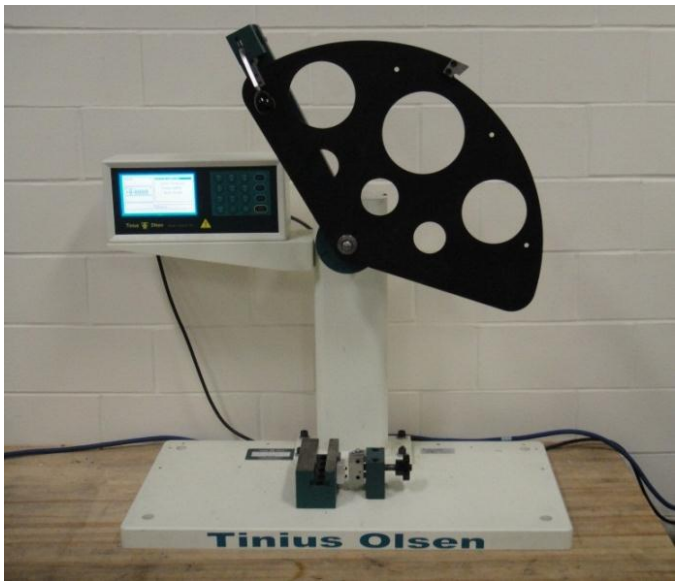

Figure 26: Tinius Olson Model Impact 104.

CHAPTER 5. RESULTS AND DISCUSSION

5.1. Density Testing

5.1.1. Areal Density

The areal density of the five mats varied considerably as shown in Table 5. The low shive flax, hemp, and kenaf were all similar at the 400-500 gsm range. This should be noted when comparing the backlit photographs in Figure 10, Figure 14, and Figure 15. The mid shive flax was roughly twice as dense as these other mats, and the high shive flax had the highest areal density at 1305 gsm, as well as the highest standard deviation. The coefficient of variation shown on the table is the standard deviation divided by the mean and is a dimensionless number. It shows that the variation in the mat is greatest in the hemp and high shive flax mats.

Table 5: Areal Density of Natural Fiber Mats.

Mat	Areal Density (gsm)		
	Average	St. Dev.	Coef. of Var.
Low Shive Flax	514	23.0	0.04
Mid Shive Flax	933	54.2	0.06
High Shive Flax	1305	137.0	0.10
Hemp	439	64.3	0.15
Kenaf	503	33.4	0.07

5.1.2. Fiber Density

The fiber densities are shown below in Table 6. The densities were similar for all samples tested with the exception of the high shive flax at 0.954 g/cm^3, which is approaching the density of the immersion fluid, canola oil, at 0.91 g/cm^3. Typically the

density of most bast fibers is in the range of 1.3-1.5 g/cm^3 [4]. The low density of the high shive flax mat can be attributed to the density measurement being an effective mat density including both fiber and shive. The presence of the large amount of shive present in the mat, and the low density of the shive, reduced the effective density. When attempting to measure the density of the shive separately from the rest of the mat, some shive was observed to float in the canola oil, and returned to the surface even after being forced below the surface. Unexpectedly, the higher shive content did not lead to a higher coefficient of variation relative to the mats with a lower shive content. All mats had similar coefficients of variation with the exception of the mid shive flax, which was twice that of the high shive flax, hemp, and kenaf mats.

Table 6: Fiber Density of Natural Fiber Mats.

Mat	Density (g/cm^3)		
	Average	St. Dev.	Coef. of Var.
Low Shive Flax	1.287	0.050	0.039
Mid Shive Flax	1.300	0.082	0.063
High Shive Flax	0.954	0.027	0.028
Hemp	1.391	0.037	0.026
Kenaf	1.331	0.040	0.030

5.2. Fiber Property Testing

5.2.1. Wax Content

The wax content for each fiber is shown below in Table 7. It was clearly the highest in the low shive flax mat at 2.12%. The mid shive flax mat was nearly half that of the low shive flax mat, with the high shive flax, hemp and kenaf lower still. Plant variety

differences and the extent of retting will influence the wax content of the fiber, but unfortunately we did not have control of this for this study.

Table 7: Wax Content of Natural Fibers.

Mat	Wax Content (%)
Low Shive Flax	2.12
Mid Shive Flax	1.09
High Shive Flax	0.87
Hemp	0.53
Kenaf	0.32

5.2.2. Fiber Thickness

The comparison of the fiber thicknesses present in each mat is shown below in Table 8. The low shive flax mat had the smallest fiber thickness at 21.78 μm, while the mid and high shive flax possessed nearly identical fiber thicknesses. The hemp and kenaf were considerably larger, with the kenaf fiber nearly 3 times as thick as the low shive flax fiber.

Table 8: Fiber Thickness of Natural Fibers.

Mat	Fiber Thickness (μm)
Low Shive Flax	21.78
Mid Shive Flax	30.57
High Shive Flax	30.88
Hemp	50.19
Kenaf	61.87

5.3. Shive Content Testing

The shive content testing showed a large variation in shive content between the three flax mats. It was not an even distribution however, with the low shive flax mat containing

4% shive, the mid shive mat containing 12% shive, and the high shive mat containing 46%. The results are shown graphically in Figure 27. As stated earlier, the NIR technique used to measure shive content is calibrated only for flax fiber. The technique could be used on the hemp and kenaf mats, but a partial least squares (PLS) model would need to be developed for each fiber type and should be the focus of a future project.

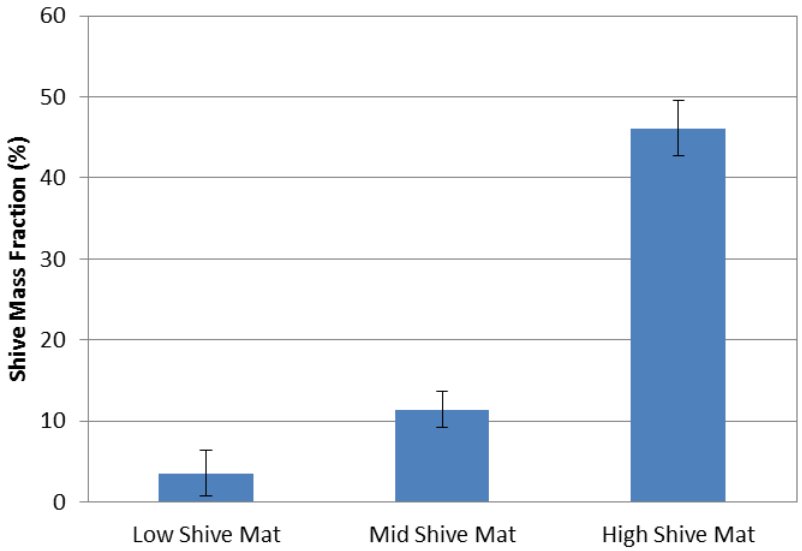

Figure 27: Shive testing results.

5.4. Compression Testing

The compression testing results for all five natural fiber mats with a fiber volume fraction of 50% are shown in Figure 28. All mats tested exhibited a rapidly increasing compression pressure followed by relaxation of the compressive pressure as detailed by Kim, et al. [23]. All natural fiber mats tested exhibited a viscoelastic response to the compaction pressure, which can be attributed to the nonwoven fiber network, as well as natural fibers being inherently viscoelastic. The kenaf mat required the greatest

compressive force to achieve a 50% fiber volume at 1720 kPa. The mid shive flax mat required the least compressive pressure at 1020 kPa.

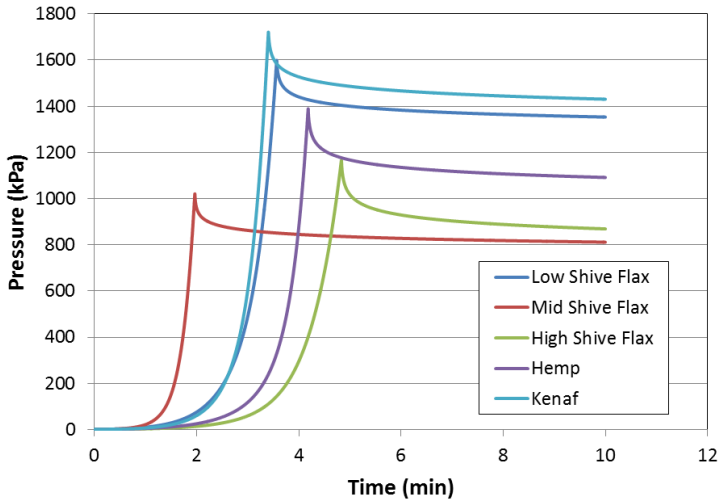

Figure 28: V_f = 50 % Compression test results.

A nonwoven fiberglass mat was also tested to compare the behavior of a nonwoven mineral fiber mat to that of a nonwoven natural fiber mat. As seen in Figure 29, both materials exhibited a rapid increase in compressive pressure as the fiber volume fraction approached 50%, and both exhibited a similar relaxation after the target thickness was reached. This again is a clear viscoelastic behavior, which can be attributed to the nonwoven fiber network as well as the light polymer binder which is used on the continuous fiber mat (CFM) fiberglass. Also, the CFM fiberglass had a much lower compaction pressure at a 50% fiber volume at only 740 kPa. The low shive flax mat shown in the figure had a maximum compaction pressure of 1600 kPa. Comparing these materials then it can be seen that greater clamping pressure is required to compress the natural fiber mat than is required by the mineral fiber. This is an important processing difference that

would need to be accounted for by a composite material manufacturer if converting a product from mineral fiber to natural fiber.

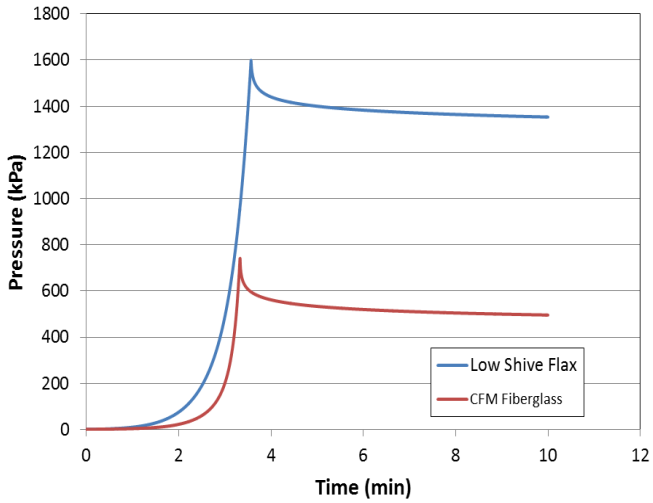

Figure 29: Compression test comparison between natural fiber and mineral fiber, V_f = 50 %.

The ratio of the compressive stress over the initial stress vs. time is shown in Figure 30. All nonwoven mats from this study as well as the CFM fiberglass mat are compared. It was observed that of the three flax mats, the high shive had the greatest relaxation after 600 s at 0.72. The mid shive flax mat was next at 0.78, and the low shive flax mat relaxed the least at 0.83. The amount of relaxation in the flax mats correlated well with the shive content, with increasing shive resulting in greater relaxation. The kenaf relaxed to 0.82 and the hemp relaxed 0.77. The CFM fiberglass had the greatest relaxation at 0.65 times the initial stress. This relaxation time must be understood by the composite processor, as the resin should not be applied until the preform has relaxed.

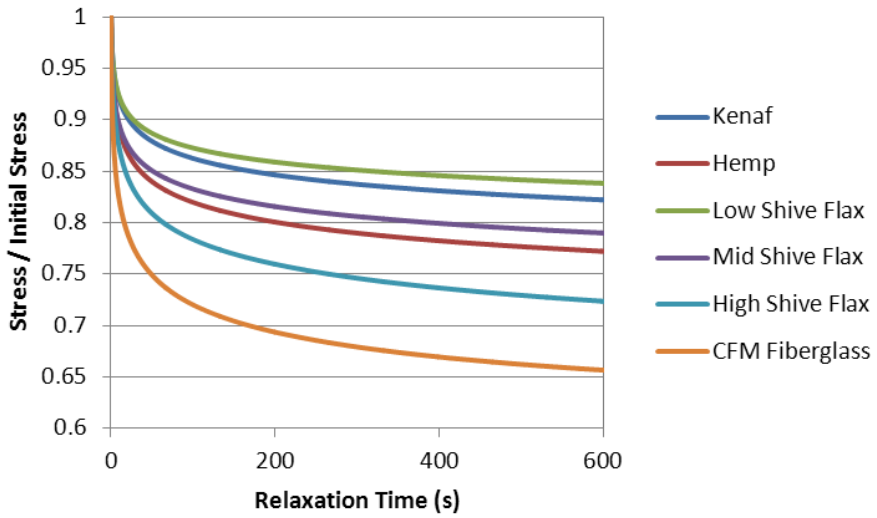

Figure 30: Stress relaxation of various nonwoven mats.

5.5. Permeability Testing

As described earlier, the instantaneous Φ (a dimensionless number related to the fluid front and the inlet diameter) was calculated using measurements taken from the video analysis. A Φ function was then fitted to the instantaneous function to determine the slope of the function. The slope of the curve was then used to calculate the permeability for the given test. Figure 31 shows the instantaneous data with the fitted function overlaid. The linear regression applied to each permeability test allowed for a simple check to confirm a good fit of the data. Any test with a poor fit was rejected, which was attributed to inconsistencies in the mats. To put it another way, these inconsistencies in the mats resulted in the quasi-isotropic conditions not being met, and therefore the isotropic model was not valid for tests with a poor fit. Table 9 shows the data from a test of the hemp mat at V_f=20% and 200 cP simulated resin with the calculated mean flow front position calculated Φ, slope m, and the R^2 value.

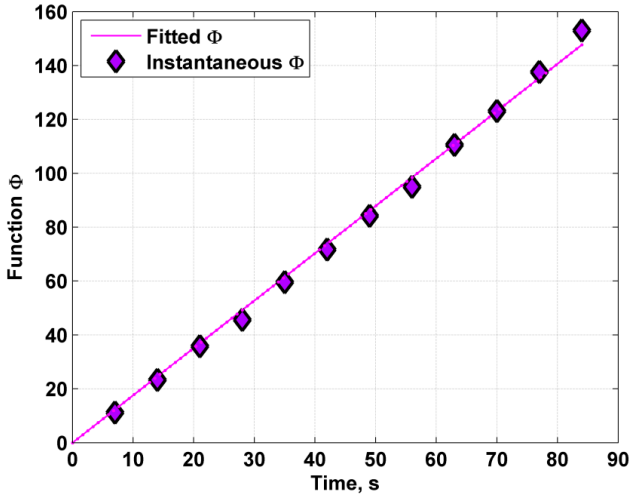

Figure 31: Sample Φ vs. time plot.

Table 9: Fluid Front Data and Φ Calculation for Hemp Mat, V_f=20%, 200 cP

Test Time (s)	Position 1 (mm)	Position 2 (mm)	Position 3 (mm)	Position 4 (mm)	Average Position (mm)	Φ
0	7	7	7	7	7	0
7	49	50	47	47	48.25	34.2
9	54	57	52	52	53.75	45.6
11	58	61	56	57	58	55.7
13	63	65	59	61	62	66.2
15	66	70	63	65	66	77.8
17	70	73	66	68	69.25	87.9
19	73	77	69	71	72.5	98.8
21	75	79	72	74	75	107.7
23	78	82	75	77	78	118.9
25	81	85	77	79	80.5	128.7
27	83	88	79	82	83	138.9

m= 7.201

R^2= 0.999

An additional check to confirm the data fit the model was to compare the mean value of radial displacement vs. time. Figure 32 shows a sample plot showing the experimental data compared to the model. Note the r/r_0 starts at 1 when time is 0 s.

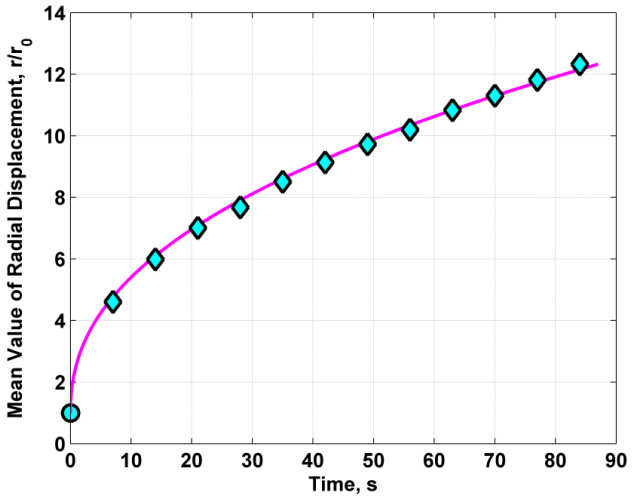

Figure 32: Sample radial displacement vs. time plot.

Figure 33 is a plot of the permeability vs. fiber volume fraction for the low shive flax mat. The plot compares the permeability values for both simulated resins. The range of fiber volume fractions tested was 16% to 32%, which is a typical range for nonwoven composite applications. The maximum permeability occurred at the 16% fiber volume, and the lowest occurred at 32% fiber volume. Also, since the density of mat was used to determine the fiber volume fraction was an effective density, the fiber volume fraction can then be said to be an effective value. The meaning of this is that the mat includes both fiber and shive, rather than just fiber, and both are accounted for in determining the density and therefore also fiber volume. The permeability results were very similar for both simulated resins. The permeability of the mat decreased and the variation of the permeability decreased as the fiber volume fraction increased.

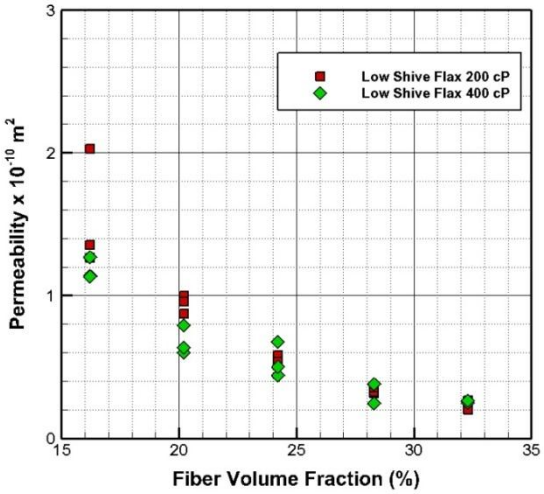

Figure 33: Permeability vs. V_f for the low shive flax mat.

The permeability vs. fiber volume fraction for the mid shive flax mat for both simulated resins is shown in Figure 34. Range of fiber volume fractions tested was from 17% to 23%. The permeability for both simulated resin viscosities was very similar, and the permeability of the mat decreased as the fiber volume fraction increased.

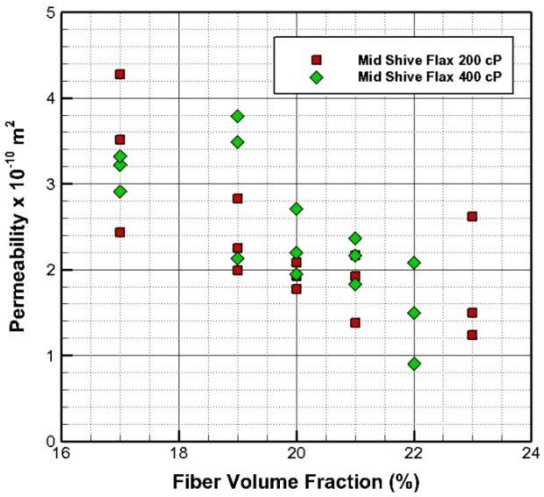

Figure 34: Permeability vs. V_f for the mid shive flax mat.

Figure 35 show the permeability vs. fiber volume fraction for the high shive flax mat with the two simulated resins. The range of fiber volume fractions tested was from 18% to 28%. Permeability decreased as the fiber volume fraction increased, and permeability was similar for both simulated resins.

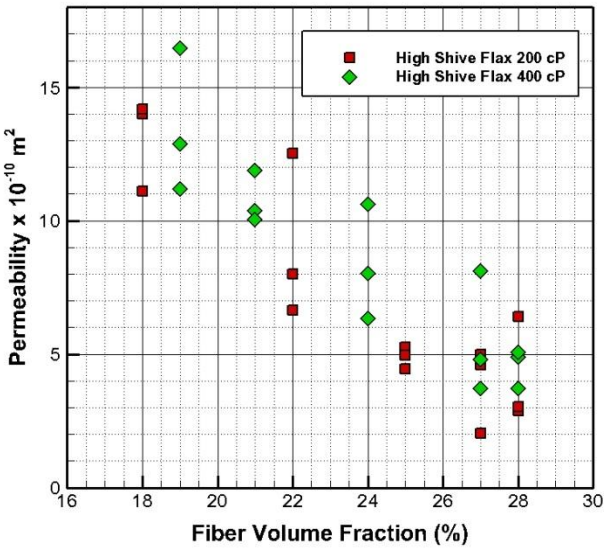

Figure 35: Permeability vs. V_f for the high shive flax mat.

Results for the permeability vs. fiber volume fraction for the hemp mat with both simulated resins are shown in Figure 36. The range of fiber volumes tested are from 14% to 32%. Again, the results for both simulated resins were very similar and the permeability decreased as the fiber volume fraction increased. This consistency for both viscosities is ideal from the perspective of the composite manufacturer. Since the permeability is the same for a given mat for different resin viscosities, the permeability would not need to be retested if a resin of a different viscosity was substituted in the process.

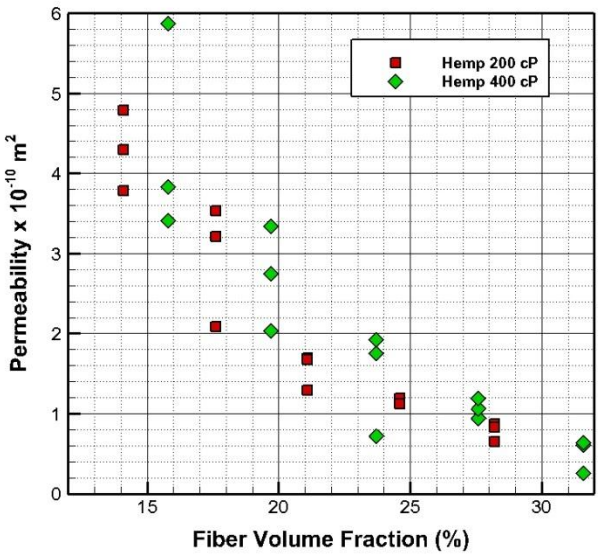

Figure 36: Permeability vs. V_f for the hemp mat.

Figure 37 shows the results for the permeability vs. fiber volume fraction for the kenaf mat. The range of fiber volumes tested was from 20% to 40% for the 200 cP simulated resin, and from 24% to 50% for the 400 cP simulated resin. The permeability was similar for both simulated resins and decreased as the fiber volume fraction increased.

Figure 38 compares the permeability of the three low trash content mats with the 200 cP simulated resin. This figure shows that the kenaf mat is the most permeable, followed by the hemp mat, and the low shive flax mat is the least permeable of the three mats. All three mats also have greater variation in the permeability at lower fiber volume fractions compared to higher fiber volume fractions. There are two important considerations for the composite manufacturer with this phenomenon. The variation in permeability at low fiber volume fractions will lead to inconsistencies in the processing, while the reduced permeability at high fiber volume fractions may require higher applied pressure to the resin to create an acceptable processing time.

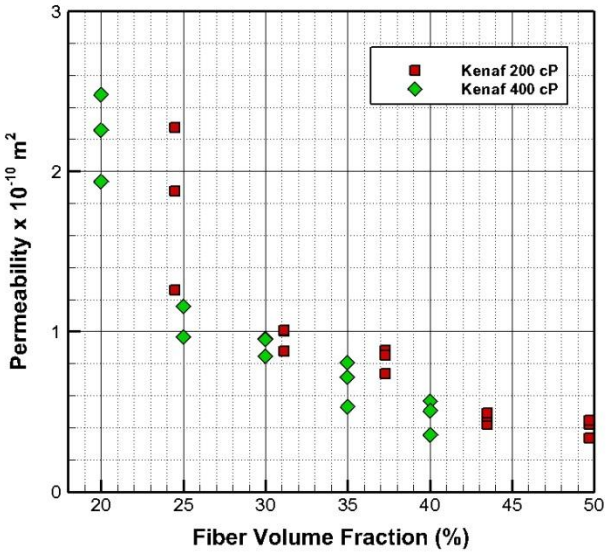

Figure 37: Permeability vs. V_f for the kenaf mat.

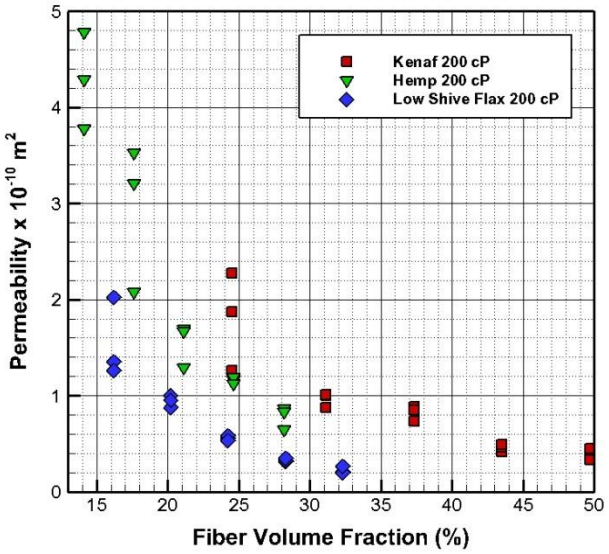

Figure 38: Permeability vs. V_f for various mats with 200 cP oil.

Figure 39 compares the permeability of the three low trash mats compared fiber volume fraction for the 400 cP simulated resin. The permeability of the hemp and kenaf mats are

very similar, and the low shive mat was found to be the least permeable of the three. The variation in the permeability was again found to be greatest at the lower fiber volume fractions.

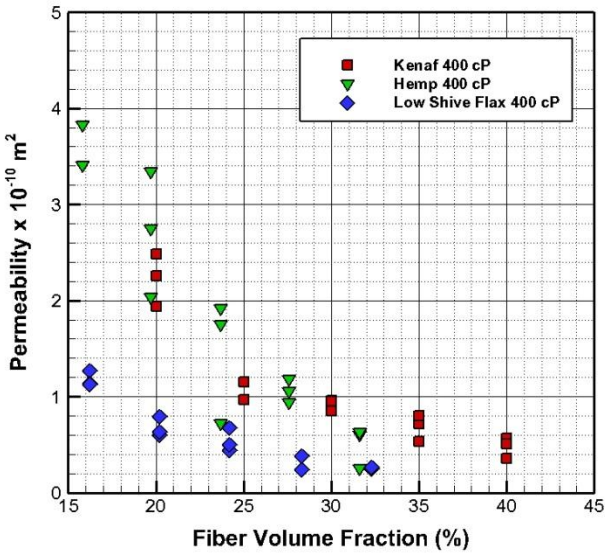

Figure 39: Permeability vs. V_f for various mats with 400 cP oil.

A comparison of the permeability for the three flax fiber mats for the 200 cP simulated resin is shown in Figure 40. The high shive flax mat was found to have by far the highest permeability as well as the greatest variation in permeability. The mid shive flax mat was the next most permeable, followed by the low shive flax mat. The variation in the low and mid shive flax mats was found to be much less than that for the high shive flax mat.

The permeability vs. fiber volume fraction for the three flax mats with 400 cP simulated resin is shown below in Figure 41. Again, the high shive flax had the highest permeability and the greatest variation in permeability. The mid shive flax mat was the next most permeable and the low shive flax mat had the lowest permeability.

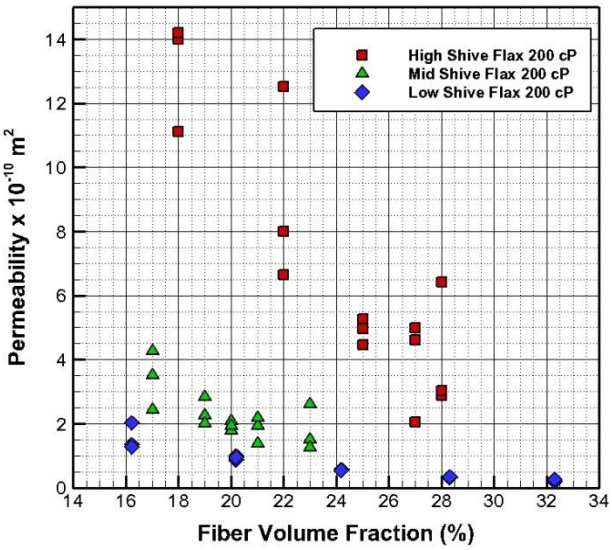

Figure 40: Permeability vs. V_f for mats with different shive quantities with 200 cP oil.

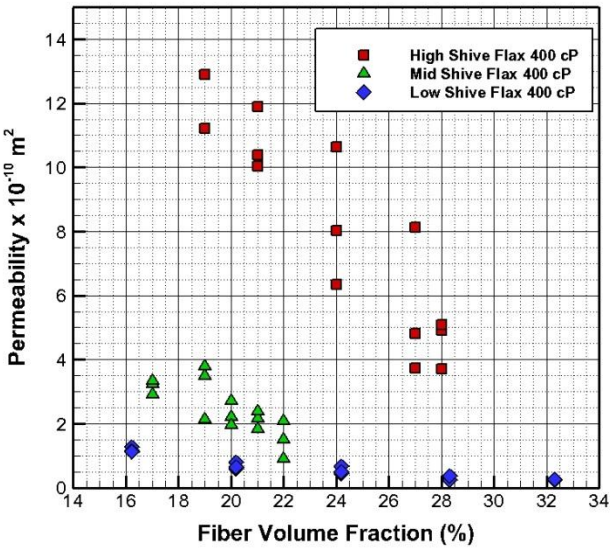

Figure 41: Permeability vs. V_f for mats with different shive quantities with 400 cP oil.

A comparison of the permeability at V_f = 20% vs. the wax content of the fibers is shown in Figure 42. Since not all of the mats were tested exactly at V_f = 20%, a fitted value

had to be used. There is a clear trend in the data showing a decrease in permeability with an increase in wax content of the fiber. Only the three low trash mats are shown in the figure because the mid shive flax and high shive flax do not fit this trend. It is hypothesized that although the wax content may affect the mid shive flax and high shive flax mats, it appears that the shive has such a great effect on permeability it cannot be observed. It is hypothesized that higher wax content would inhibit resin wetting on the surface of the fibers. It is for this reason that the wetting behavior was measured in the form of contact angle and is discussed in the following section.

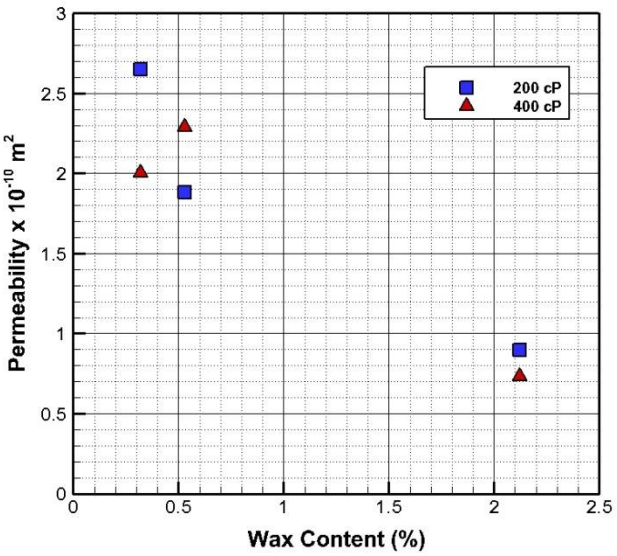

Figure 42: Permeability at V_f = 20% vs. wax content for low trash mats.

Figure 43 shows a comparison of the permeability at V_f = 20% to the fiber size for the low trash mats. There is a clear trend showing an increase in permeability with an increase in fiber size. Only the three low trash mats exhibited this behavior, as it appears again that the shive content has such a great effect on permeability this trend cannot be observed. The trend of greater fiber size being associated with higher permeability could be attributed to

the larger fibers not packing in as tightly, resulting in larger channels for the resin to flow between the fibers. Conversely the smaller fibers will pack in tighter, resulting in smaller channels for the resin to flow and lower permeability.

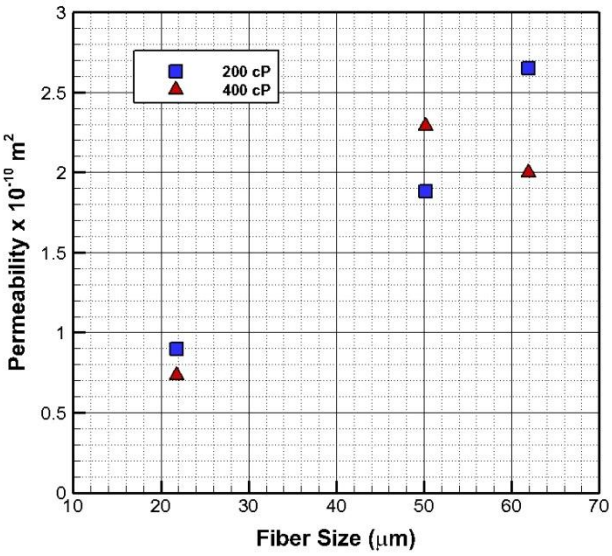

Figure 43: Permeability at V_f = 20% vs. fiber size for low trash mats.

5.6. Wettability Testing

All of the fibers tested showed an average higher contact angle for the higher viscosity oil except for the high shive flax mat fiber. This likely occurs due to the slight differences in chemical makeup of the oil which creates slight differences in the polarity matchup with the oil and the surface chemistry of the fibers. The high shive flax fiber showed no appreciable difference in contact angle between the two oils. The largest variation was found for the kenaf fiber with the 400 cP oil. The least amount of variation was found with the low shive flax fiber and the 200 cP oil. The mid shive flax fiber exhibited the highest contact angle for both the 200 cP oil and the 400 cP oil.

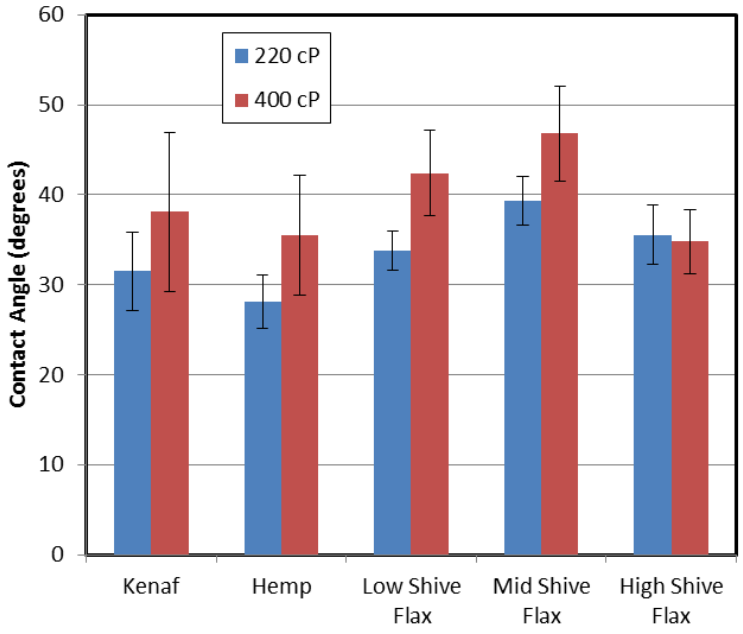

Figure 44: Contact angle test results.

The contact angle of the shive could not be determined using the same procedure as the fiber. Approximately half of all contact angle measurements on the shive resulted in the oil droplet being absorbed by the woody material, and thus having no measureable contact angle. The shive particles that did not absorb the oil appeared to be cuticle or an intact stalk, as seen in Figure 45. Since the contact angle of the shive could not be measured, its effect is not accounted for in the wettability portion of this study.

When comparing permeability to contact angle for all mats, as seen in Figure 46, no clear trend is obvious. The clear outlier is the high shive flax mat, which occurs at approximately 10 x 10^{-10} m^2 and 12 x 10^{-10} m^2. Since shive content appears to be much more influential than contact angle on permeability, both the mid and high shive flax mat data are removed from Figure 47, which compares the permeability vs. contact angle for only the low trash mats.

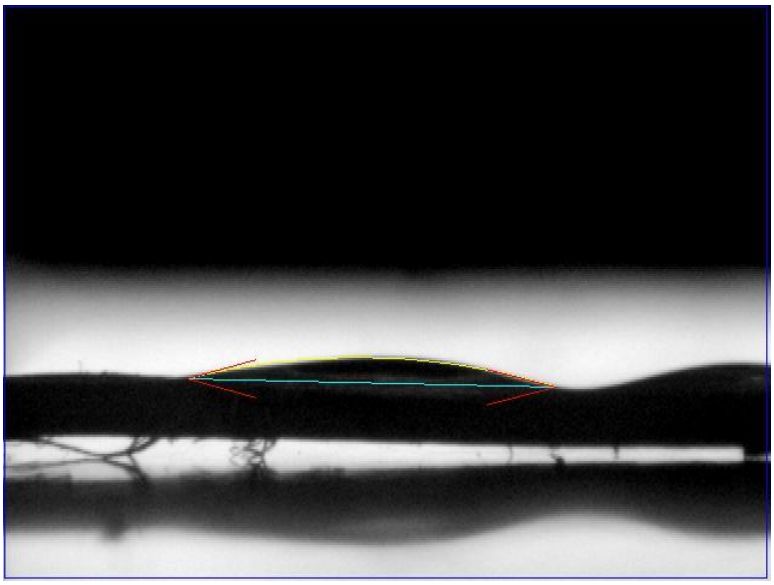

Figure 45: Contact angle measurement of flax shive.

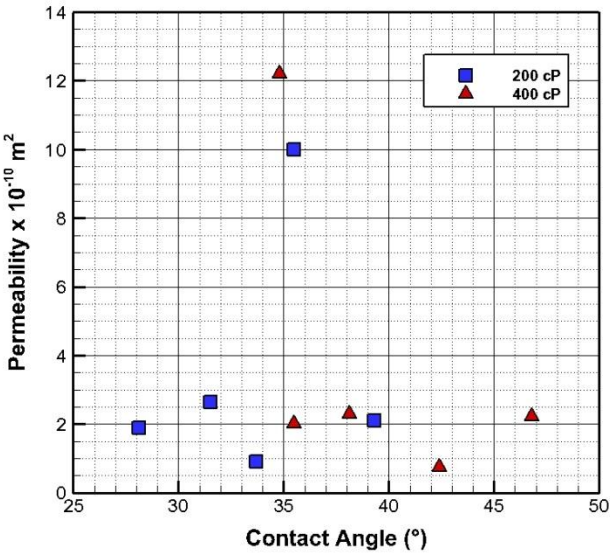

Figure 46: Permeability vs. contact angle for all mats.

Figure 47 does indicate a slight trend of decreasing permeability with an increase in contact angle for the low trash mats at V_f = 20%. This trend is exhibited in the 400 cP oil between the limited number of data points. The 200 cP oil however does not exhibit this trend as clearly. The permeability vs. contact angle for the low trash mats at V_f = 40% is

shown in Figure 48. This was examined to observe if the contact angle had a greater effect on the permeability when the porosity is decreased and the fibers are in closer proximity to one another. There is not as clear of a trend for the 200 cP simulated resin, but again the 400 cP resin shows a very clear trend of decreasing permeability with an increase in contact angle. It appears then that the poorer wettability decreases the permeability, which is analogous to reducing the capillary pressure. This supports the findings that an increase in wax content will result in a decrease in permeability due to the poorer wettability.

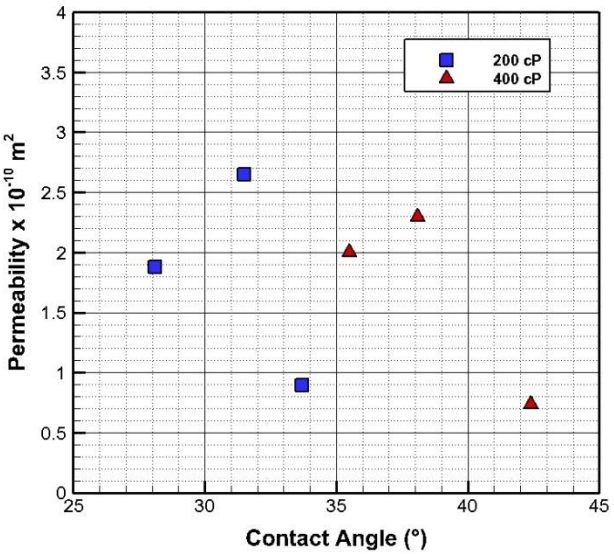

Figure 47: Permeability at V_f = 20% vs. contact angle for low trash mats.

In order to determine the applicability of the simulated resins in the area of contact angle testing, the simulated resin contact angle measurements were compared to that of several commercial resin systems. The test was performed only on the low shive flax fiber. The results are shown below in Figure 49. The contact angle for the three resins was very similar to the 200 cP simulated resin. The standard deviation of the three commercial resins was also slightly greater than that for the two simulated resins. The similarity of the contact

angle for the commercial resins to that of the simulated resins confirms that the use of simulated resins is a valid approach.

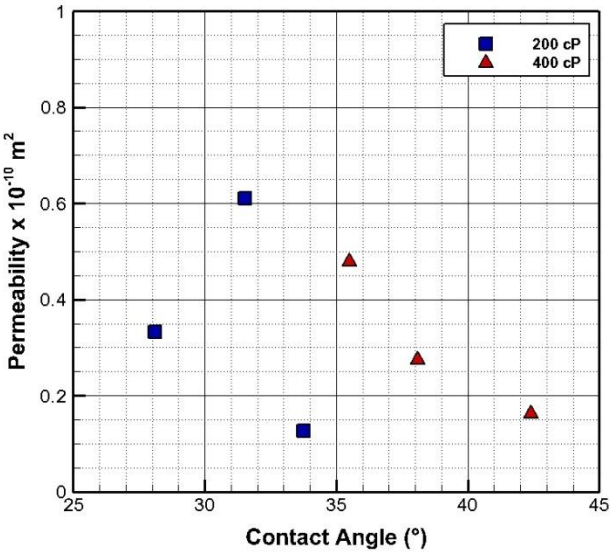

Figure 48: Permeability at V_f = 40% vs. contact angle for low trash mats.

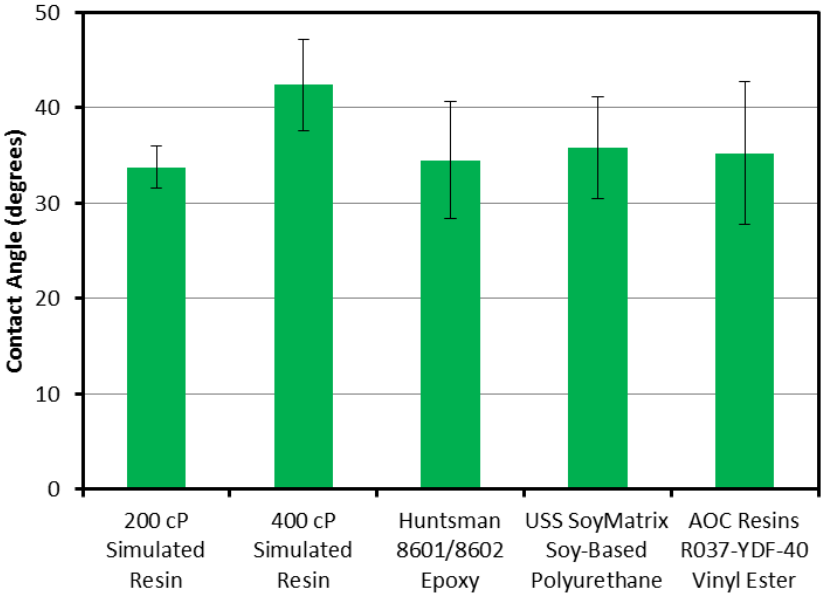

Figure 49: Contact angle for simulated resins and various commercial resins on low shive flax.

5.7. Cross Section of Flax Fiber Composites

In order to better understand the effect of the shive on the permeability of the three flax mats, cross section samples were created for each of the three mats at 20% and 30% fiber volume fractions. The samples were created by compressing the mats to the desired thickness, followed by an infusion of an epoxy resin with 6% green pigment to create plaques. The pigment was used to make the matrix stand out from the fiber. A sample was then cut from each plaque and placed in an epoxy holder. The samples were then wet sanded with 120, 200, 320, 400, and 600 grit sandpaper. The photographs of each cross section were taken at 4 times magnification.

5.7.1. Low Shive Flax Cross Section

The low shive flax cross sections are shown below in Figure 50 and Figure 51. Only a small amount of shive is present in each figure, with large separation between the shive shown.

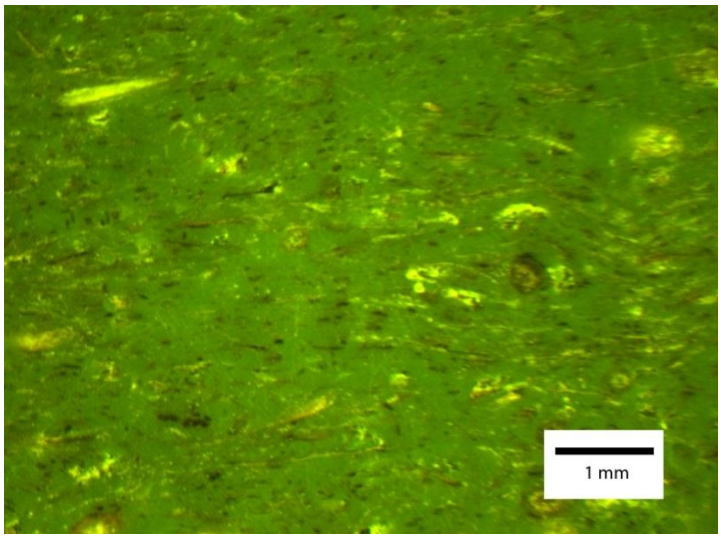

Figure 50: Low shive flax cross section, $V_f = 0.20$.

The fibers are visible in both figures as the black and brown specs. The fibers appear to be distributed evenly throughout the cross section of both samples. There is also a large piece of shive, which appears to be an entire plant stalk in Figure 51.

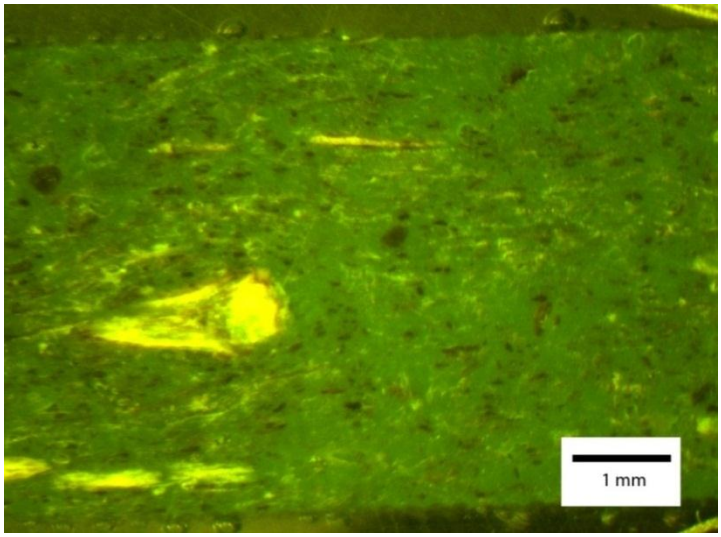

Figure 51: Low shive flax cross section, $V_f = 0.30$.

5.7.2. Mid Shive Flax Cross Section

The cross section samples for the mid shive flax mat are shown in Figure 52 and Figure 53. Compared to the low shive flax cross sections, there is a clear increase in shive content for both the 20% and 30% fiber volume fraction. There appears to be an even distribution of fibers throughout the cross section not occupied by shive.

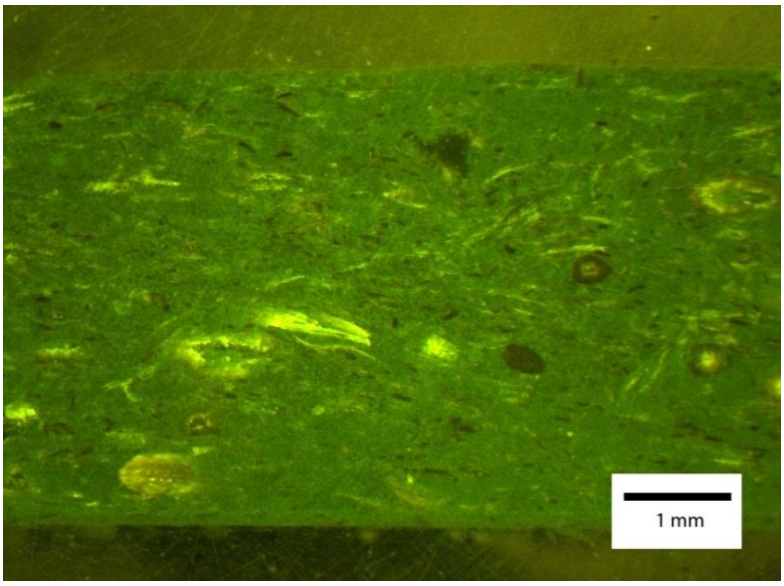

Figure 52: Mid shive flax cross section, $V_f = 0.20$.

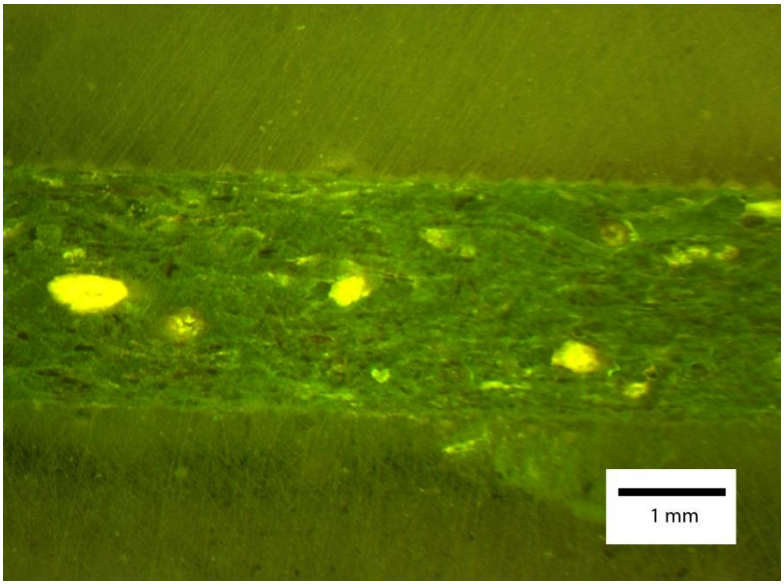

Figure 53: Mid shive flax cross section, $V_f = 0.30$.

5.7.3. High Shive Flax Cross Section

The high shive flax mat cross sections are shown in Figure 54 and Figure 55. There is a large amount of shive visible in both figures, with the shive in direct contact with other

shive in some spots. The majority of the shive in both figures appears to be entire plant stalks, with multiple stalks clearly cross sectioned in both figures.

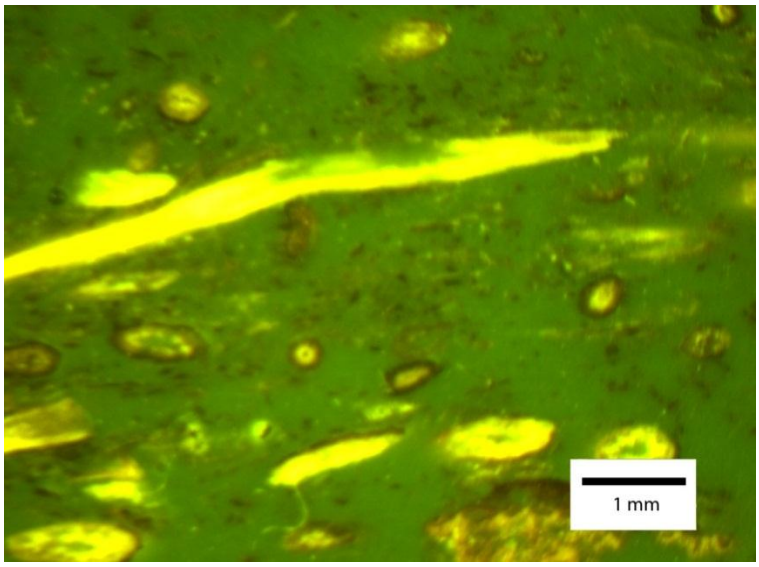

Figure 54: High shive flax cross section, $V_f = 0.20$.

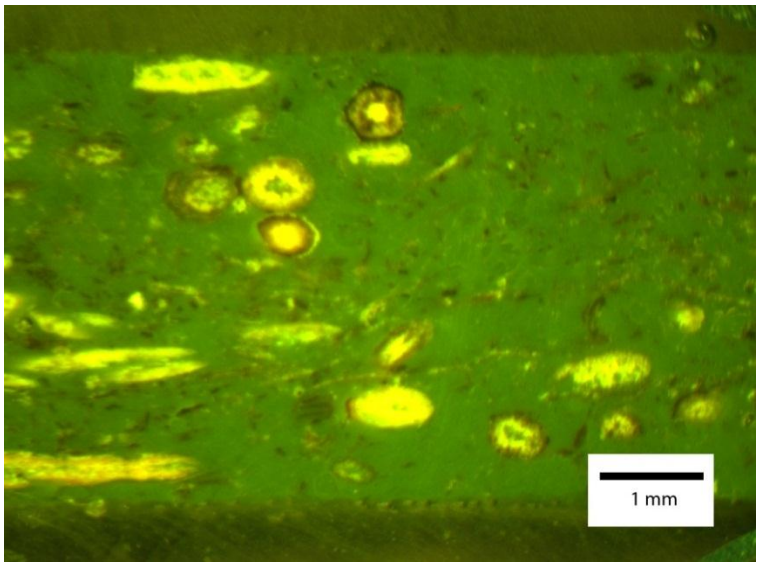

Figure 55: High shive flax cross section, $V_f = 0.30$.

Another interesting feature in both figures is the variation of fiber concentration, with both high and low concentrations. These areas of low fiber concentration are in effect areas

of high porosity, which would act as channels for the flow of resin throughout the mat. The combination of the presence of whole plant stalks as well as the variation in fiber concentration illustrate the low quality of the mat, and it should be mentioned again that the purpose of this mat in this study was to provide a large contrast between the low and high shive mats in order to discern the influence of shive content on permeability.

5.8. Mechanical Property Testing

The low trash mats were tested for tensile, flexural and impact properties to compare the performance of different bast fibers. The mid shive flax mat and the high shive flax mat were not evaluated in this part of the study.

5.8.1. Tensile Testing

The tensile strength of the natural fiber reinforced soy-based PU as well as the neat PU is shown in Figure 56. The tensile strength for all three composites were very similar. Fiber volume fraction for the three composites was also similar; the low shive flax panel had a fiber volume fraction of 40.5%, the kenaf panel had a fiber volume fraction of 34.6%, and the hemp panel had a fiber volume fraction of 37.3%. All three bast fiber types exhibited improved performance over the neat resin, proving load transfer and the reinforcing effect of these fibers in the soy-based PU resin.

Figure 57 shows the elastic modulus for the natural fiber PU composites as well as the neat PU. The hemp was found to be the stiffest, the low shive flax was less stiff, and the kenaf was the least stiff composite. The kenaf composite also had the lowest fiber volume fraction, but the hemp composite did not have the highest fiber volume fraction. With the hemp exhibiting a higher modulus than the low shive flax, coarseness of the fibers may

play a role in the increased stiffness. Void content may also be affecting the data and will be explored in a future study.

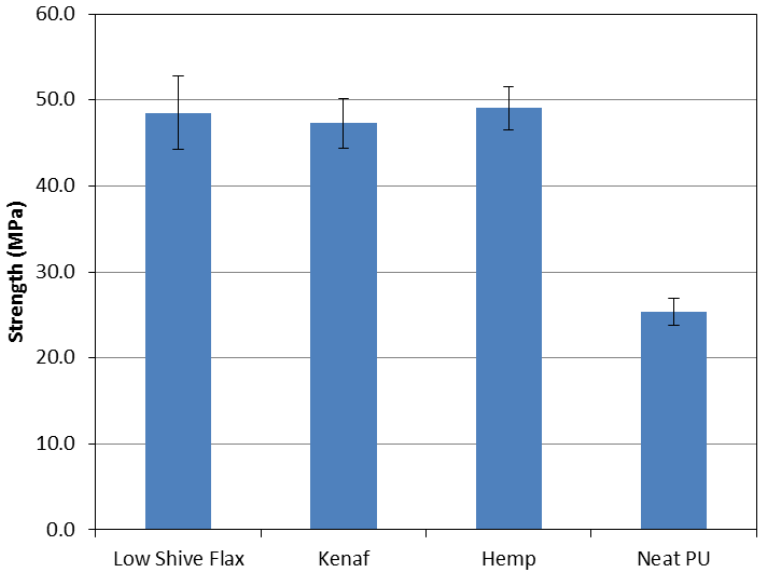

Figure 56: Tensile strength of natural fiber PU composites and neat PU.

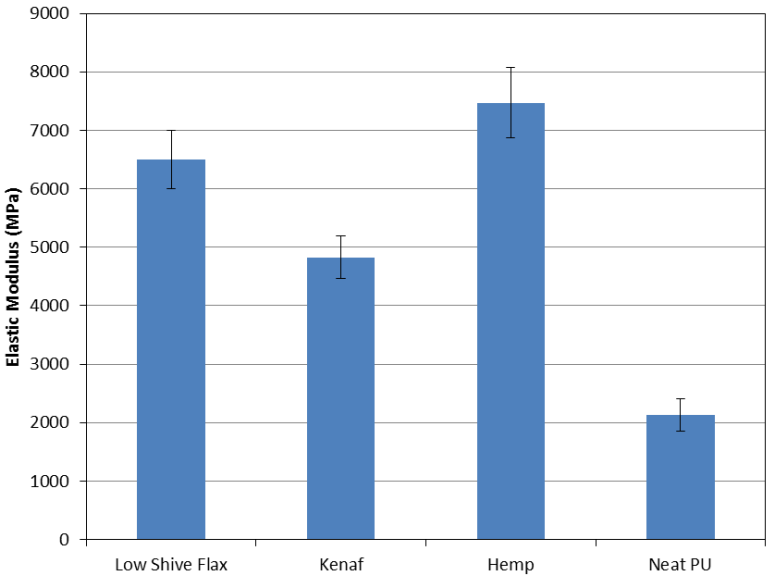

Figure 57: Elastic modulus of natural fiber PU composites and neat PU.

5.8.2. Flexural Testing

The results of the flexural strength for the natural fiber PU composites and the neat PU are shown in Figure 58. Fiber volume fraction for the three panels was similar; the low shive flax panel had a fiber volume fraction of 38.6 %, the kenaf panel had a fiber volume fraction of 33.5 %, and the hemp panel had a fiber volume fraction of 36.8 %. The hemp had the highest strength followed by the kenaf. The low shive flax was the weakest of the three composites, and it also had the greatest variation. The coarser fibers appear to be performing better, which may be due to the thinner fibers buckling under the compressive load.

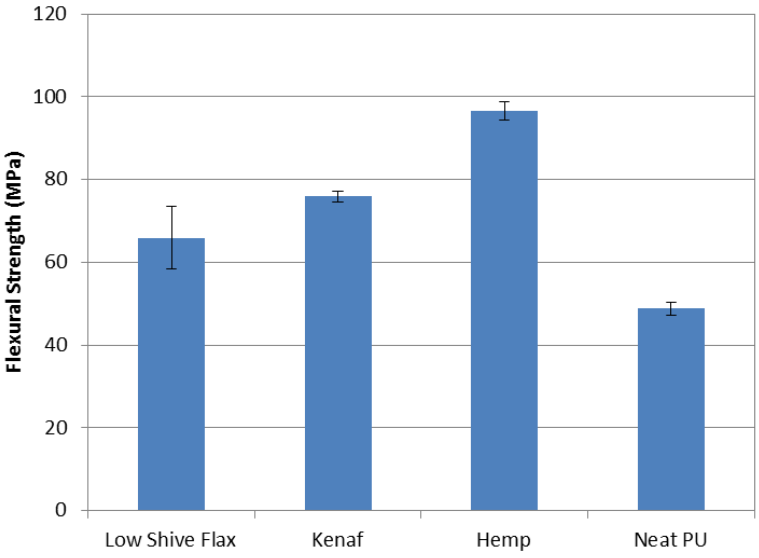

Figure 58: Flexural strength of natural fiber PU composites and neat PU.

The flexural modulus for the three composites and the neat PU is shown in Figure 59. The hemp composite was the stiffest, and the low shive flax and kenaf composites were less stiff and very similar. The behavior among the three fiber types is similar for both the

flexural strength and flexural modulus to the tensile elastic modulus results, except for the higher low shive flax value. Also, all fiber reinforced PU composites performed better than the neat PU proving that load transfer is occurring and the fibers are not merely acting as filler. It is also interesting that the hemp fiber performed the best of the three fibers, and hemp also has the lowest contact angle. The hemp fiber could be attaining a superior bond to the PU due to higher surface energy, thus providing improved load transfer and the best performance.

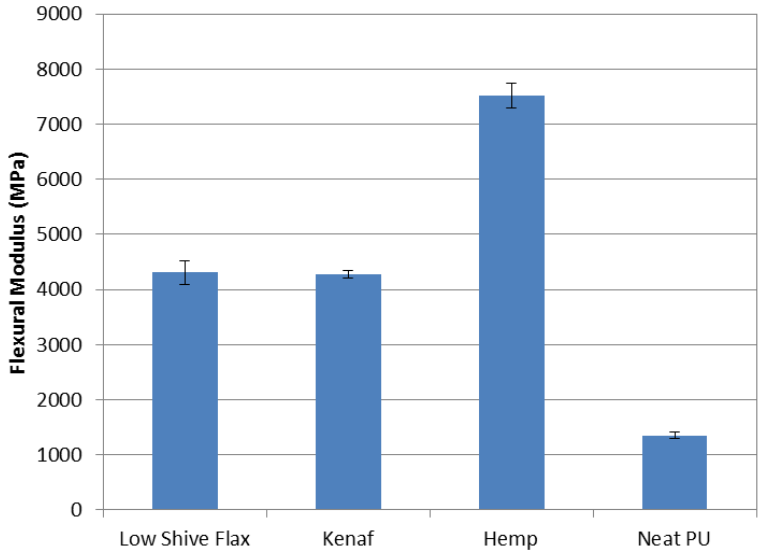

Figure 59: Flexural modulus of natural fiber PU composites and neat PU.

5.8.3. Impact Testing

The results of the impact testing are shown below in Figure 60. Fiber volume fraction for the three panels was similar; the low shive flax panel had a fiber volume fraction of 35.4 %, the kenaf panel had a fiber volume fraction of 30.3 %, and the hemp panel had a fiber volume fraction of 32.1 %. The hemp fiber composite had the superior impact strength, followed by the kenaf and the low shive flax. It is possible that the coarser fibers

in the hemp and kenaf composites provide more modes of failure (i.e. fiber pull out, fibril separation, fibril fracture, etc.) and therefore increased energy absorption during an impact event.

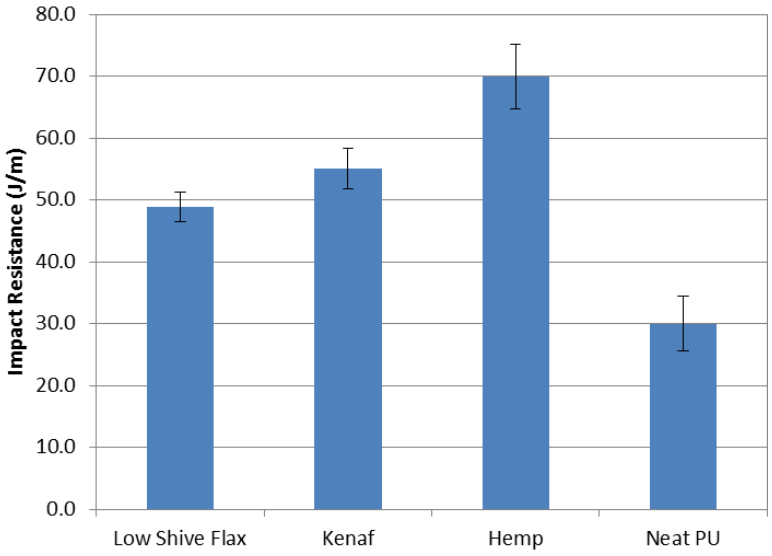

Figure 60: Impact resistance of natural fiber PU composites and neat PU.

CHAPTER 6. CONCLUSIONS AND RECOMMENDATIONS

This chapter covers the conclusions reached during the course of this research. In the interest of expanding on this research and improving experimental techniques, a future recommendation section is also included.

6.1 Mat Compression

The nonwoven natural fiber mats exhibited relaxation characteristics similar to other nonwoven materials, including mineral fibers. The shive content appears to influence the amount of relaxation of the mat, with higher amounts of shive correlating with greater relaxation, and lower amounts of shive correlating with less relaxation. The only nonwoven fiberglass mat tested exhibited greater relaxation than any of the natural fiber mats tested. This was expected due to the viscoelastic bonding polymer applied to the fiberglass mats. Also, some of the natural fiber mats required twice the compressive pressure to achieve the same fiber volume fraction as the mineral fiber mat evaluated.

6.2 Permeability

All mats tested showed a decrease in permeability with an increase in fiber volume fraction, consistent with previous studies on mineral and synthetic based fiber mats. The natural fiber mats studied also showed similar permeability results for both the 200 cP oil and the 400 cP oil. This may be due to the similarity of the viscosity of the two oils, and further investigation of the viscosity on the permeability would require a greater viscosity difference. A greater difference in the oils could also provide a greater difference in the chemical makeup of the oil, which would affect the polarity matchup between the oil and the natural fibers.

Shive content greatly influenced the permeability of the flax mats. The high shive mat had the highest permeability of the three flax mats and the greatest variation. The low shive flax mat had the lowest permeability of the three and the lowest variation. This was likely due to the larger channels for the resin to flow that the shive created in the mat.

An increase in wax content of the fibers of the low trash mats correlated with a decrease in permeability, while an increase in fiber diameter correlated with an increase in permeability. Also, an increase in contact angle correlated with a decrease in permeability. These relationships were only exhibited for the low trash mats. The mid shive flax and high shive flax mats fell outside of all of these trends. This is likely due to the shive content having a greater influence on the permeability than these other fiber properties. It can be stated then that the order of importance for factors influencing permeability in this study then are first shive, followed by fiber size, wax content, and contact angle. However, as the fluid pressure is decreased, the capillary effect will become more important, which would likely increase the effect of wax content and contact angle on permeability.

In order to produce a natural fiber mat with improved permeability, a low wax content fiber should be used with a larger fiber diameter and a smaller contact angle. The single greatest parameter in a natural fiber mat observed in this study however was shive or trash content of the mat. Trash does not appear to reinforce composite materials as well as bast fiber, however, and mechanical properties would decrease as the shive content of the mat increased. These competing factors could be used by a mat manufacturer to produce a mat which had optimum permeability while still maintaining acceptable strength.

6.3 Mechanical Properties

The natural fiber PU composites exhibited similar ultimate strengths but were otherwise dissimilar, and all composites outperformed the neat PU material. This shows that for all composites there was matrix to fiber adhesion and load transfer. The hemp fiber PU composite was the stiffest, absorbed the most energy, and had equal tensile strength among all of the composites tested. The low shive flax PU composite was the second stiffest composite under tensile loading, but performed the poorest in flexural strength, flexural stiffness and impact. The low shive flax mat had the smallest fiber size, highest wax content, and lowest permeability. It is unclear, but speculated that some, if not all of these characteristics played a role in the decreased mechanical performance.

6.4 Future Work

Further investigation for permeability includes examining the influence of mat construction on permeability. The parameters to be tested for this would include adjusting the air-lay parameters as well as the amount needle punching while maintaining the same fiber feedstock. This study would require access to a consistent fiber feedstock, as well as access to a mat construction line and good control of such parameters.

Another potential study would be to control the amount of shive in a mat in order to achieve optimal permeability. This study could also use the same fiber feed stock throughout a series of mats in order to control the variables of wax content and fiber size, compared to the current study. Mechanical testing could also be performed on these samples to determine the effects of shive on mechanical properties of natural fiber composites.

In order to further explore wetting of natural fiber mats and compare wetting characteristics to permeability, other wetting measurements should be examined. In particular, experimentation using the capillary rise method or the Wilhelmy plate method should be pursued. These methods of measurement would better account for the wettability of the entire mat using a measurement technique which is applied to the entire mat. This would account for the effect of the shive or hurd on the wettability, rather than just measuring that of the fiber. Another interesting study to examine the effect of contact angle would be to test samples of a mat with different surface treatments and compare the results of the contact angle and permeability. This should allow for the evaluation of a greater range of contact angles while controlling many other variables.

REFERENCES

[1] G. Bogoeva-Gaceva et al., "Natural Fiber Eco-Composites," *Polymer Composites*, pp. 98-107, 2007.

[2] S. V. Joshi, L. T. Drzal, A. K. Mohanty, and S. Arora, "Are natural fiber composites environmentally superior to glass fiber reinforced composites?," *Composites: Part A 35*, pp. 371-376, 2004.

[3] C.A. Ulven, I.S. Akhatov, E. Jerke, E. Kerr-Anderson S. Mekic, "Evaluation of in-plane and transverse permeability of flax fiber preforms for biocomposite materials," *Journal of Biobased Materials and Bioenergy*, vol. 3, no. 2, pp. 156-164, 2009.

[4] A. K. Mohanty, M. Misra, and G. Hinrichsen, "Biofibres, biodegradeable polymers, and biocomposites: An overview," *Macromolecular Materials and Engineering*, vol. 276-277, no. 1, pp. 1-24, 2000.

[5] X. Li, L.G. Tabil, and S. Panigrahi, "Chemical treatments of natural fiber for use in natural fiber-reinforced composites: a review," *Journal of Polymers and the Environment*, vol. 15, no. 1, pp. 25-33, 2007.

[6] W. Van Cotthem and E. Fryns-Claessens, "Plantenanatomie in Praktijk," *Publ. Van In Leir*, p. 195, 1972.

[7] B.E. Palleson, "The quality of combine-harvested fibre flax for industrials purposes depends on the degree of retting," *Industrial Crops and Products 5*, pp. 65-78, 1996.

[8] C. Van Sumere, "Retting of flax with special reference to enzyme-retting," in *The biology and processing of flax*. Belfast, Northern Ireland: M Publications, 1992, pp.

153-193.

[9] D.E. Akin, J.A. Foulk, R.B. Dodd, and D.D. McAlister III, "Enzyme-retting of flax and characterization of processed fibers," *Journal of Biotechnology 89*, pp. 193-203, 2001.

[10] M. Alcock, M. Fuqua, C.A. Ulven, E. Kerr-Anderson, and J. Foulk, "A comparison of fibre characteristics between linseed flax, canadian grown linen flax and european linen flax with respect to performance as a composite reinforcement," in *International Conference on Flax and Other Bast Plants*, 2008, pp. 258-269.

[11] C. Pouteau, S. Baumberger, B. Cathala, and P. Dole, "Lignin-polymer blends: evaluation of compatibility by image analysis," *Comptes Rendus Biologies 327*, pp. 935-943, 2004.

[12] J. N. Jagannadh and F. Kolla, "An update - Canadian oilseed flax straw utilisation," in *Tappi Pulping Conference*, San Francisco, CA, 1997.

[13] D.E. Akin, D.S. Himmelsback, and W.H. Morrison III, "Biobased fiber production: Enzyme retting for flax/linen fibers," *Journal of Polymers and the Environment*, vol. 8, no. 3, pp. 103-109, 2000.

[14] W. Albrecht, H. Fuchs, and W. Kittelmann, *Nonwoven Fabrics*. Weinheim, Germany: Wiley-VCH, 2003.

[15] S. Mekic, *Porous Media Characterization Applied to Fiber Reinforcements and Membranes*. Fargo, ND: North Dakota State University, 2008.

[16] L. T. Drzal, M. J. Rich, and W. Ragland, "Adhesion between fiber and matrix - its effect on composite test results," in *42nd Annual Conference, Composite Institute, The*

Society of Plastic Industries, 1987.

[17] I. Aranberri-Askargorta, T. Lampke, and A. Bismarck, "Wetting behavior of flax fibers as reinforcement for polypropylene," *Journal of Colloid and Interface Science 263*, pp. 580-589, 2003.

[18] J. G. Williams, C.E.M. Morris, and B. C. Ennis, "Liquid flow through aligned fiber beds," *Polymer Engineering and Science*, vol. 14, no. 6, pp. 413-419, June 1974.

[19] A. Pietak, S. Korte, E. Tan, A. Downard, and M.P. Staiger, "Atomic force microscopy characterization of the surface wettability of natural fibers," *Applied Surface Science 253*, pp. 3627-3635, 2007.

[20] J.L.G. Silva and H.A. Al-Qureshi, "Mechanics of wetting systems of natural fibers with polymeric resin," *Journal of Materials Processing Technology 92-93*, pp. 124-128, 1999.

[21] A. Krishnan et al., "An evaluation of methods for contact angle measurement," *Colloids and Surfaces B: Biointerfaces 43*, pp. 95-98, 2005.

[22] K.J. Ahn, J. C. Seferis, and J. C. Berg, "Simultaneous measurements of permeability and capillary pressure of thermosetting matricies in woven fabric reinforcements," *Polymer Composites*, vol. 12, no. 3, pp. 146-152, June 1991.

[23] Y.R. Kim and S.P. McCarthy, "Compressibility and Relaxation of Fiber Reinforcements During Composite Processing," vol. 12, no. 1, 1991.

[24] "ASTM D3039-00 Standard Test Method for Tensile Properties of Polymer Matrix Composite Materials,".

[25] "ASTM D790-03 Standard Test Methods for Flexural Properties of Unreinforced and

Reinforced Plastics and Electrical Insulating Materials,".

[26] "ASTM D256-06 Standard Test Methods for Determining the Izod Pendulum Impact Resistance of Plastics,".

[27] S. Mekic, C.A. Ulven, and I. Akhatov, "Report on Permeability Measurement of CIC Natural Fiber Mats," Fargo, ND 58102,.